Electronic Supplementary Material (ESI) for Chemical Science.

Supporting Information

Tunable Helicity, Stability and DNA-Binding Properties of Short Peptides with Hybrid Metal Coordination Motifs

Sarah J. Smith, Robert J. Radford, Rohit H. Subramanian, Brandon R. Barnett, Joshua S. Figueroa and F. Akif Tezcan

Department of Chemistry and Biochemistry, University of California, San Diego, 9500 Gilman Dr., La Jolla, California 92093-0356

Table of Contents

I. General Considerations

a. Supplies

Unless otherwise stated, reagents and solvents were purchased from Fisher Scientific and used as received. Supplies for peptide synthesis (amino acids and resins) were purchased from Aapptec and used without further purification.

b. HPLC purification

Reverse-phase HPLC was performed using 0.1% trifluoroacetic acid (TFA) in water as buffer A and acetonitrile as buffer B. Newly synthesized peptides were purified on a preparative-scale column (Agilent preHT, 5 µm, 21.1 x 100 mm) on an Agilent Technologies 1260 Infinity HPLC instrument; chromatograms were monitored at 220 nm to detect absorbance of the peptide backbone and fractions were collected manually. Preparative scale purifications were run at a flowrate of 6 mL/min using a gradient of 0 to 60% buffer B over 40 min. Phen-conjugated peptides were purified using the same column and methods, monitoring the absorbance at 268 nm. After initial purification, an analytical column (Agilent Eclipse plus C_{18}, 3.5 µm, 4.6 x 100 mm) was run using an isocratic gradient from 10 to 40% buffer B over 15 min with a flow rate of 1 mL/min to determine purity. All peptides were isolated to >90% purity and the masses were verified using MALDI-TOF mass spectrometry.

c. Mass Spectrometry

Mass spectrometry analysis was carried out at the Molecular Mass Spectrometry Facility at UC San Diego. Peptide mass spectrometry was performed on a Bruker Bioflex IV MALDI-TOF mass spectrometer. Typically, peptides were diluted to 1-10 µM in water, and combined with 50% by volume α-cyano-4-hydroxycinnamic acid (CHCA) (Agilent) as a matrix. 3 µL of the peptide-matrix solution was then spotted on a standard 288-well plate and the sample was dried before analysis.

Small molecule mass spectrometry was performed using electrospray ionization (ESI) on a Quattro Ultima Triple Quadrupole mass spectrometer. Samples were diluted to a concentration of 0.1-1.0 mg/mL using a solution of 50% methanol in water. Analysis was performed using both positive and negative ion modes.

II. Synthesis of 5-iodoacetamido-1,10-phenanthroline

5-iodoacetamido-1,10-phenanthroline (IPhen) was synthesized as previously. [1-3]

III. Peptide Synthesis

a. General protocols for Solid Phase Peptide Synthesis

Peptides were synthesized using an Aapptec Focus XC peptide synthesizer and standard FMOC chemistry, as previously described.[4] All peptides were *N*-terminal acylated and *C*-terminal amidated.

For each amino acid addition, the FMOC protecting group on the *N*-terminus of the growing peptide chain was first removed with a solution of 20% (v/v) 4-methylpiperidine in dimethylformamide (DMF). A 4-fold excess of an FMOC-protected amino acid containing a free *C*-terminus was then added in a solution of 4 M *N,N*-Diisopropylethylamine (DIPEA) in DMF with an equimolar amount of HATU and coupling was allowed to proceed for 40 min with shaking. The resin was then washed with DMF and the cycle was repeated until all amino acids were incorporated. After the final step of synthesis, the *N*-terminus of each peptide was acylated with a mixture of 0.5 M acetic acid anhydride, 0.5 M *N*-hydroxybenzaldehyde (HOBt) and 10% (v/v) dichloromethane in DMF.

The peptide resin was removed from the synthesizer and dried *in vacuo*. The peptide was then cleaved from the resin using a cleavage cocktail containing 5% (v/v) thioanisole, 3% (v/v) ethane dithiol and 2% (v/v) anisole in trifluoroacetic acid (TFA) over a period of two hours. After cleavage was complete, the peptide solution was filtered to remove the resin and the filtrate was added to a solution of cold ether and incubated at -80 °C overnight to precipitate the peptide from solution. The solution was then filtered, the peptide was collected as a precipitate, and dried *in vacuo*. The crude solid was redissolved in water, and purified via HPLC.

b. Functionalization of peptides with 5-iodoacetamido-1,10-phenanthroline

The synthetic schemes were adopted from previous reports.[3, 4] (Scheme S2)

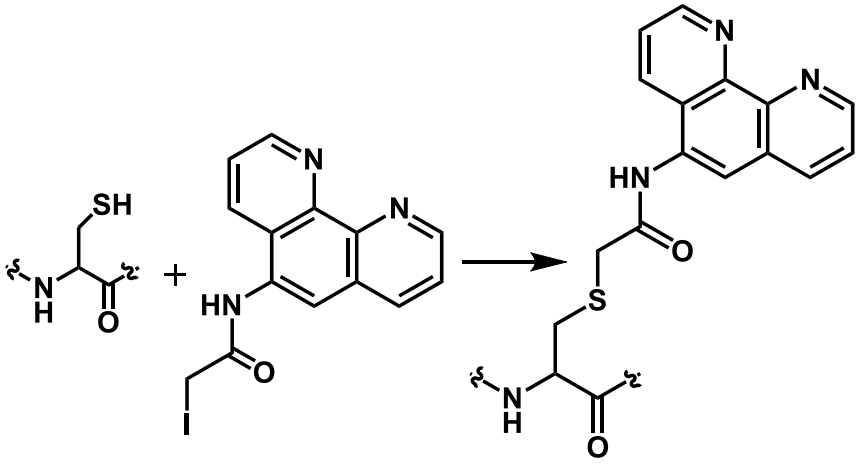

Scheme S1. Synthetic scheme for the functionalization of a peptide cys residue with 5-iodoacetamido-1,10-phenanthroline.

Under an argon atmosphere, 20 mg of each peptide was dissolved in 3 mL of degassed 10 mM HEPES buffer (pH 7.5) with constant stirring. A 3- to 5- fold excess of 5-iodoacetamido-1,10-phenanthroline (IPhen) was dissolved in 1 mL degassed DMF and added dropwise to the peptide solution.

The mixture was stirred in the dark for approximately 4 hr at room temperature. Any precipitant was removed by centrifugation, and a PD MidiTrap G-10 desalting column (GE Healthcare) was used to remove excess IPhen and DMF. The crude peptide solution was purified by preparative scale HPLC as previously described, and the identity of the labeled peptide was confirmed by MALDI-TOF mass spectrometry (Fig. S1).

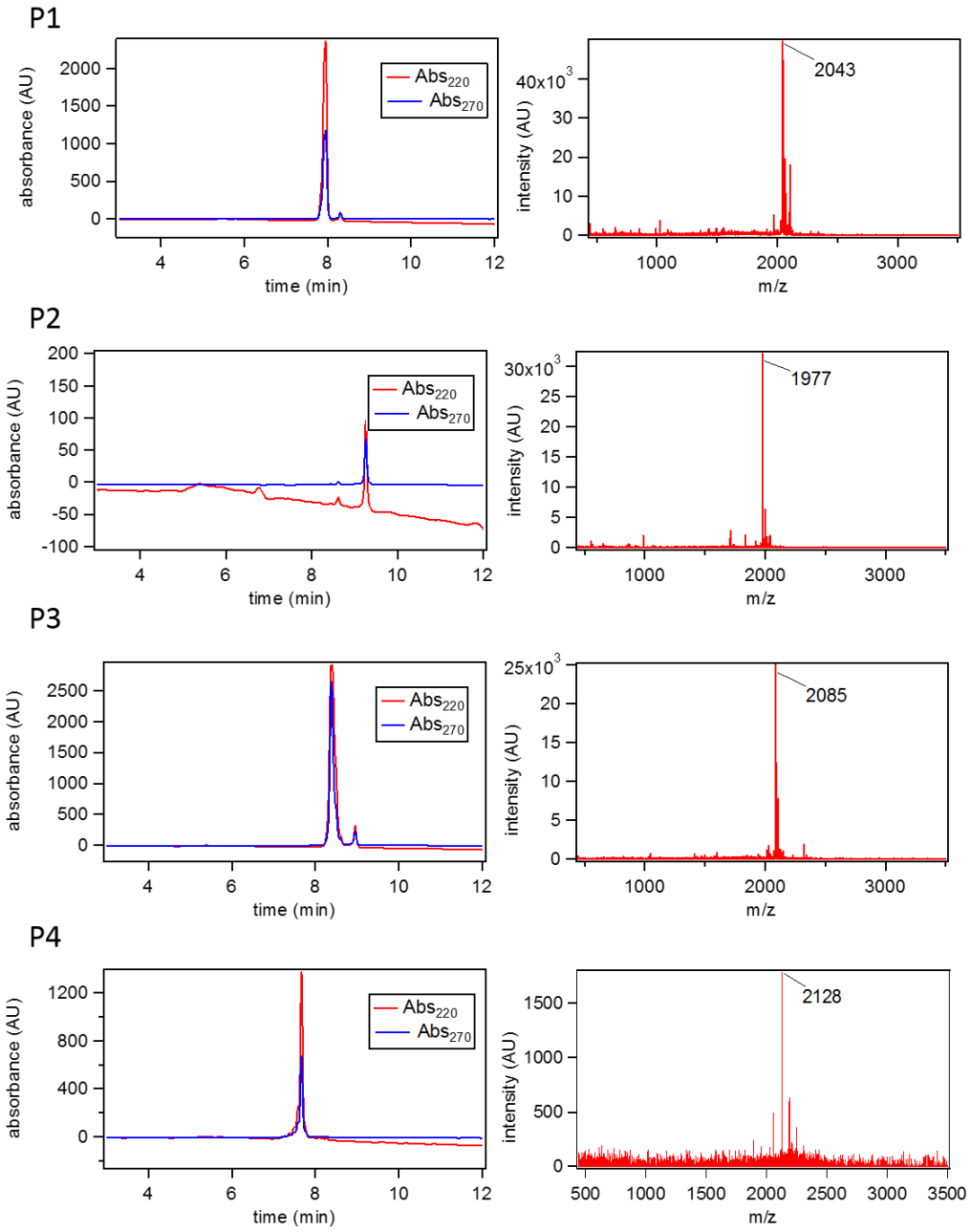

Figure S1. Analytical HPLC traces and MALDI-TOF spectra of various peptide constructs. HPLC gradient used: 1. 0 to 5 min, 90% solvent A, isocratic. 2. 5 to 20 min, 90% to 60% solvent A, linear gradient. P1: expected 2043 amu, observed 2043 $[M+H]^+$. P2: expected 1977 amu, observed 1977 $[M+H]^+$. P3: expected 2085 amu, observed 2085 $[M+H]^+$. P4: expected 2128 amu, observed 2128 $[M+H]^+$. P5: expected 2158 amu, observed 2159 $[M+H]^+$. P6: expected 2087, observed 2086 $[M+H]^+$. P7: Expected 2069, observed 2070 $[M+H]^+$. P8: Expected 4020, observed 4022 $[M+H]^+$.

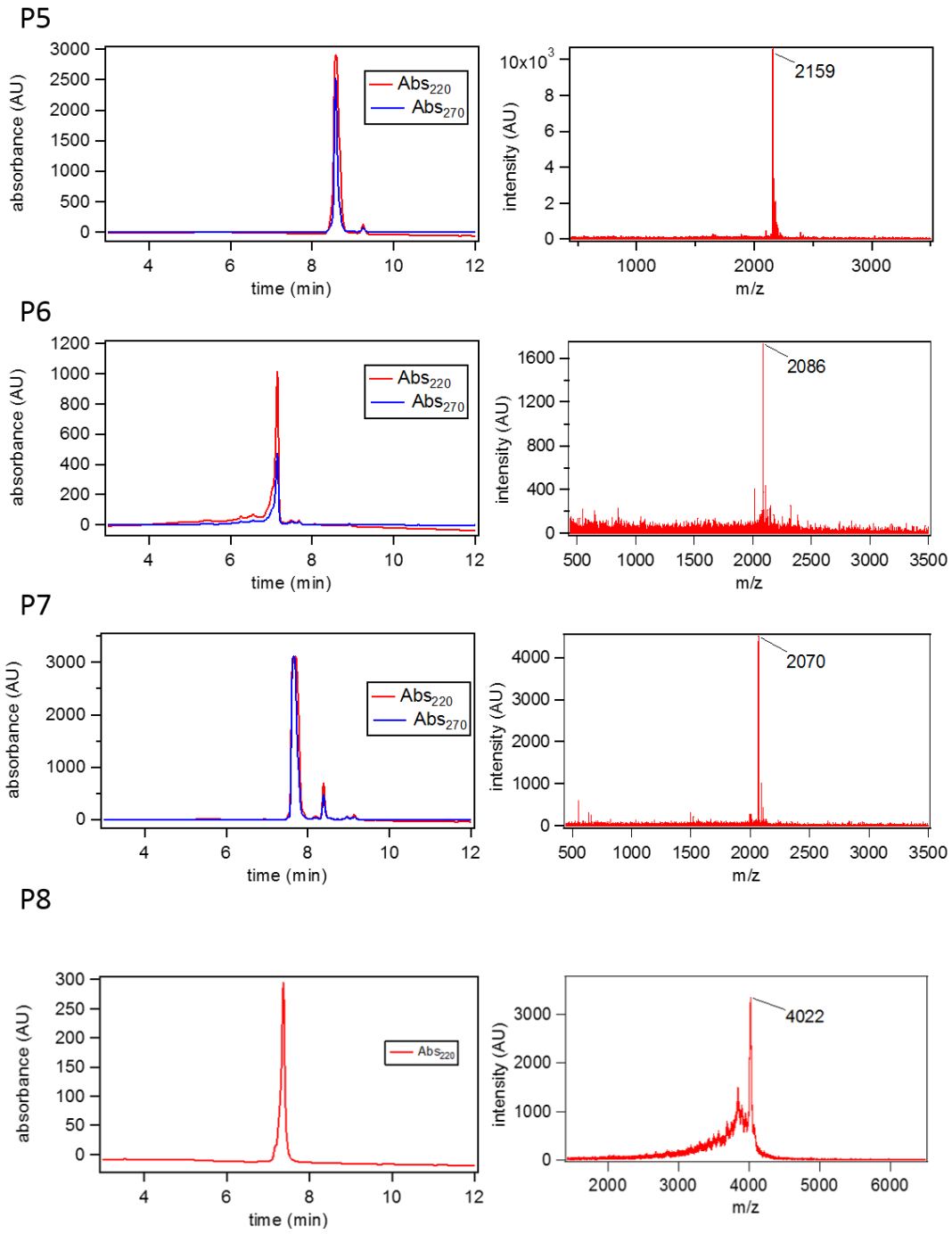

Figure S1. Analytical HPLC traces and MALDI-TOF spectra of various peptide constructs. HPLC gradient used: 1. 0 to 5 min, 90% solvent A, isocratic. 2. 5 to 20 min, 90% to 60% solvent A, linear gradient. P1: expected 2043 amu, observed 2043 $[M+H]^+$. P2: expected 1977 amu, observed 1977 $[M+H]^+$. P3: expected 2085 amu, observed 2085 $[M+H]^+$. P4: expected 2128 amu, observed 2128 $[M+H]^+$. P5: expected 2158 amu, observed 2159 $[M+H]^+$. P6: expected 2087, observed 2086 $[M+H]^+$. P7: Expected 2069, observed 2070 $[M+H]^+$. P8: Expected 4020, observed 4022 $[M+H]^+$.

IV. Determination of Metal Binding Affinity

Metal binding titrations were performed by monitoring the Phen π-π* absorption band, which shifts approximately 6 nm from 268 nm when metal-free to 274 nm when metal-bound (Fig. S2). 1 mL samples were prepared containing 10-20 μM peptide; peptide concentrations were determined more precisely using the extinction coefficient ε_{268} = 16,000 M^{-1} cm^{-1}. Each sample was prepared in 50 mM 3-(*N*-morpholino)propanesulfonic acid (MOPs) buffer, pH 7.0 pretreated with Chelex resin (BioRad) with a 3-fold excess of chelator (30-60 μM). All pipet tips were rinsed 3 times with analytical grade 10% nitric acid (Fluka) before use. The chelator used as a competing ligand depended on the binding affinity of the peptide; ethylene glycol tetraacetic acid (EGTA) was used as a competitor for Ni^{II} and Co^{II} samples, while nitrilotriacetic acid (NTA) was used for the Zn^{II} and Cu^{II} titrations. 2 mM metal stocks were prepared and added stepwise to the peptide solution so that the total amount never exceeded 5% (50 μL) of the total volume. After the addition of each aliquot, the sample was incubated for at least 3 min with constant stirring. UV-vis measurements were performed on a Hewlett Packard 8452A diode array spectrophotometer, or an Agilent 8453 UV-visible spectroscopy system. The largest changes in absorbance were measured at 280 nm, and these values were plotted as a function of M^{II} concentration after the spectra were background and dilution corrected (Fig. S2, S3). M^{II} dissociation constants for either EGTA or NTA were calculated using MaxChelator (http://maxchelator.stanford.edu) and fixed during data fitting (Table S1). The titration data were separately fit to two models using non-linear regression through Dynafit 4 (Biokin),[5] where one model assumes a 1:1 peptide:metal stoichiometry while the other model takes account of the possibility of metal-induced peptide dimerization (1:1 and 2:1 peptide:metal stoichiometry) (Scheme S3, Scheme S4, Fig. S3, Table S2) (See also Table 1).

Table S1. Dissociation constants of chelators used as competing ligands for UV-vis titrations to measure the metal binding affinity for peptide-HCMs. MaxChelator was used to determine chelator:metal dissociation constants (25 °C, pH 7.0, 0.02 M ionic strength).

Chelator	**Metal**	**K_d (M)**
EGTA	Ni^{II}	4.548×10^{-10}
EGTA	Co^{II}	7.789×10^{-9}
NTA	Zn^{II}	6.8×10^{-9}
NTA	Cu^{II}	2.18×10^{-11}

Table S2. Dissociation constants for peptide-metal complexes and metal-mediated dimers.

Metal	**K_d of His-phen HCM (M)**	**K_d of dimerization (M)**	**K_d Phen[6] (M)**
Co^{II}	$3(2) \times 10^{-8}$	$1(2) \times 10^{-6}$	8.0×10^{-8}
Ni^{II}	$3(2) \times 10^{-11}$	$2(4) \times 10^{-4}$	3.9×10^{-8}
Cu^{II}	$6(5) \times 10^{-13}$	$3(3) \times 10^{-5}$	2.5×10^{-9}
Zn^{II}	$1.7(7) \times 10^{-8}$	$1.6(7) \times 10^{-6}$	3.7×10^{-7}

(6) Martell, A. E.; Smith, R. M. *Critical Stability Constants*; Plenum Press: New York, 1974.

$$P + M \rightleftharpoons PM \quad (1)$$
$$C + M \rightleftharpoons CM \quad (2)$$
$$PM + P \rightleftharpoons D \quad (3)$$

Scheme S2. Equations used to model the metal-binding equilibria, where P is the peptide, M is the metal, C is the chelator, and D is a metal-mediated peptide model. Equations (1) and (2) only are used to fit data where only peptide-metal binding is accounted for, and all three equations are used to model a 1:1 and 2:1 binding equilibria.

```
(a)
[task]
task = fit
data = equilibria

[mechanism]
p + m <==> pm          kd1 dissoc
e + m <==> em          kd2 dissoc

[constants]
kd1 = 9e-10 ?
kd2 = 7.789e-9


[concentrations]
p = 15e-6 ?            ; M
e= 50e-6               ; M

[responses]
pm = .5e4 ?

[data]
variable m
```

```
(b)
[task]
task = fit
data = equilibria

[mechanism]
p + m <==> pm          kd1 dissoc
e + m <==> em          kd2 dissoc
pm + p <==> d          kd3 dissoc

[constants]
kd1 = 1e-11 ?
kd2 = 7.789e-9
kd3 = 1e-4 ?

[concentrations]
p = 19.3e-6 ?          ; M
e= 50e-6               ; M

[responses]
pm = .35e4
d = 2 * pm

[data]
variable m
```

Scheme S3. Dynafit scripts for describing metal-peptide binding equilibria. Two models for fitting were tried, as it is expected that a metal-mediated dimer will form at limiting metal concentrations. Metal-chelator dissociation constants were obtained via MaxChelator at pH 7.0, 25 °C, and 0.02 ionic strength and held fixed. The peptide concentration was calculated using an extinction coefficient of 16,000 cm^{-1} M^{-1}. The variables used include: peptide (p), metal (m), peptide-metal complex (pm), metal-induced peptide dimer (d), chelator (e), and metal-chelator complex (em). Parameters allowed to float during the fitting process are followed by "?" and all other parameters were held fixed. In the scripts below, (a) accounts for a 1:1 peptide:metal competitive binding model, and (b) takes into account metal-induced peptide dimerization with a 1:1 and 2:1 peptide:metal competitive binding model.

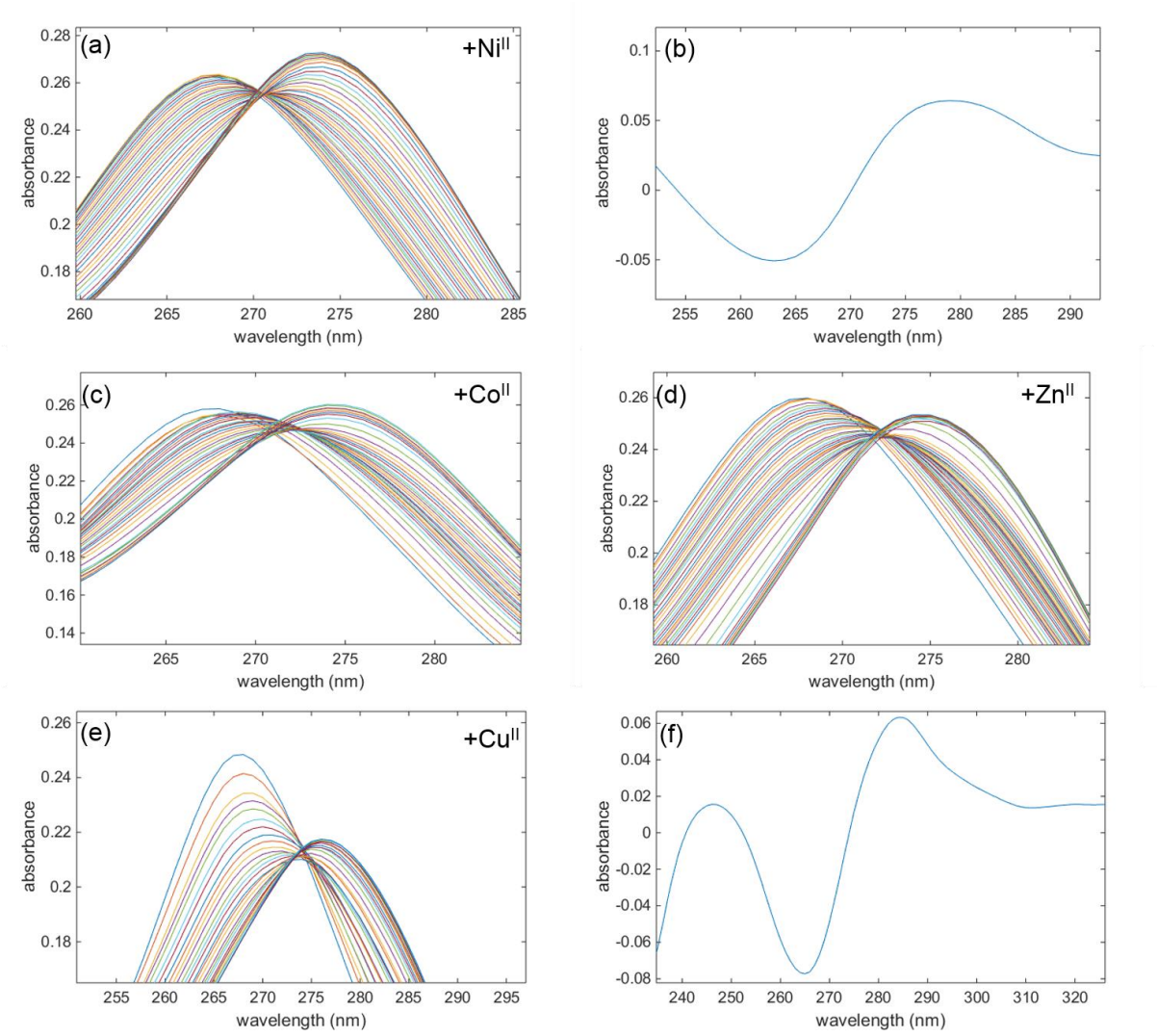

Figure S2. UV-vis spectra changes upon Phen-M^{II} coordination. Solutions were prepared with approximately 15 µM peptide and 50 µM chelator (EGTA in the case of Ni^{II} and Co^{II}, and NTA in the case of Zn^{II} and Cu^{II}), and increasing amounts of M^{II} were added by titration. A red shift in the phen π-π* transition occurs, shifting the absorbance maximum approximately 8 nm from 268 nm to 276 nm. For Ni^{II}, Co^{II}, and Zn^{II}, the increase in signal at 280 nm was used for fitting. For Cu^{II}, a larger transition was observed for the decrease at 268 nm, so this data was used for fitting. (a) The spectral shift as a result of Ni^{II} binding. (b) The difference spectrum between the metal-free peptide and the final spectrum of the Ni^{II} titration, showing the increase in the signal at 280 nm. (c) The spectral shift as a result of Co^{II} binding. (d) The spectral shift as a result of Zn^{II} binding. (e) The spectral shift as a result of Cu^{II} binding. (f) The difference spectrum for the Cu^{II} titration showing the greater change at 268 nm.

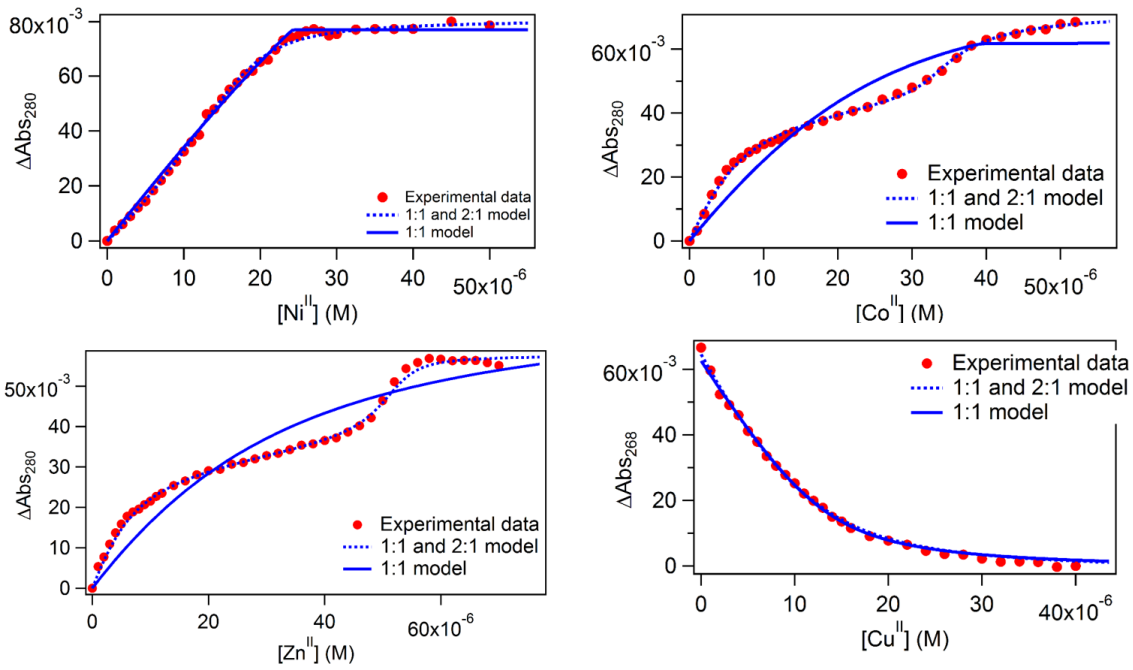

Figure S3. Peptide-metal binding isotherms and fits. Example titrations of P1 with Co^{II}, Ni^{II}, Cu^{II}, and Zn^{II} as monitored by UV-vis spectroscopy. Two different models were used for fitting, taking into account either a 1:1 peptide:metal binding stoichiometry (solid blue line) or both a 1:1 and 2:1 peptide:metal binding stoichiometry (dotted blue line), accounting for the possibility of a metal-induced peptide dimer. Overall, the 1:1 and 2:1 model fit the data better, indicating that a peptide dimer is likely forming in solution at limiting metal concentrations. In the case of Cu^{II}, the decrease in absorbance at 268 nm was fit to determine the binding affinity, while the increase in absorbance at 280 nm was used to fit the other three metals.

V. Analysis of Metallated Peptides

Mass spectrometry was performed to analyze the metal-bound peptide species using electrospray ionization (ESI) on a Quattro Ultima Triple Quadropole mass spectrometer. Samples were prepared with 100 µM peptide in water incubated with 1 equiv. of Ni^{II}, Co^{II}, or Cu^{II}, or 2 equiv. Zn^{II}. Samples were then diluted with water to a final concentration of 10 µM prior to analysis, and analyzed using 50% methanol and 0.5% acetic acid in water. Analysis was performed using positive ion mode.

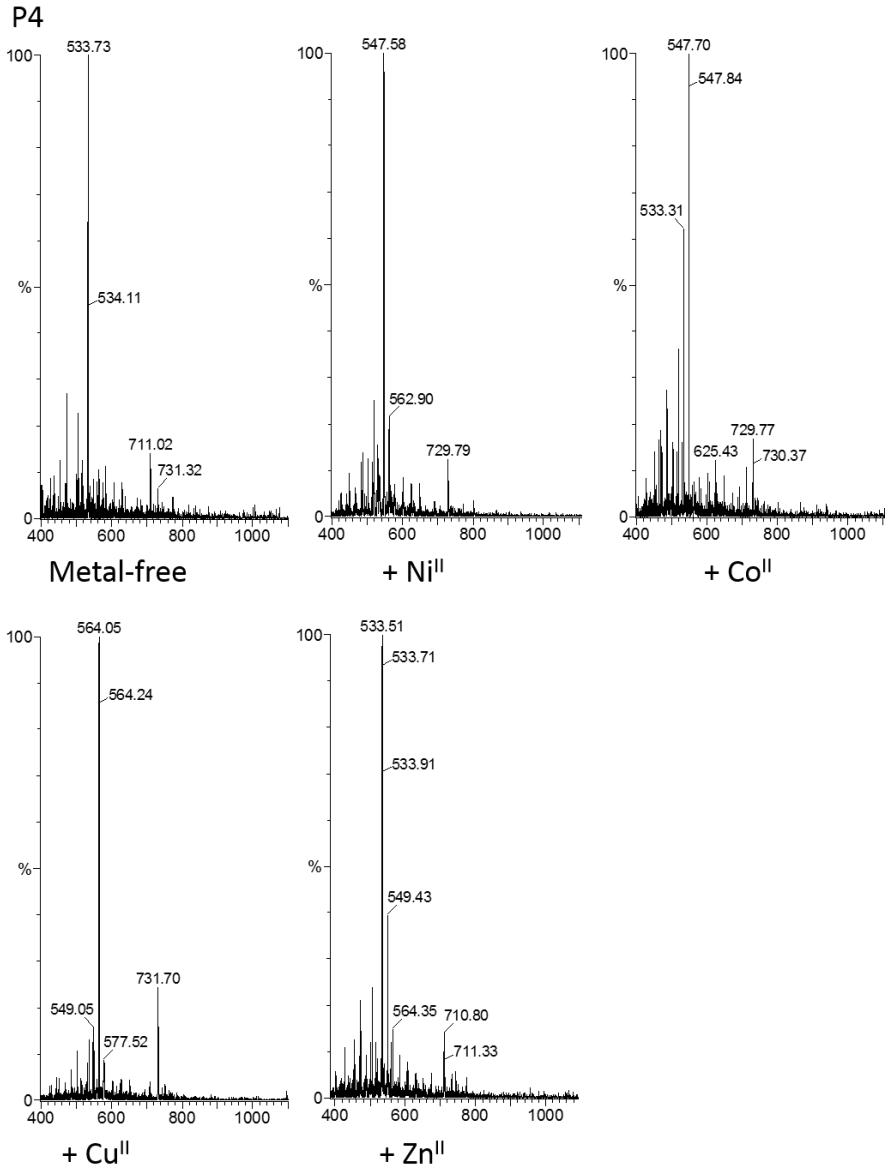

Figure S4. ESI spectra of metallated P4.

Table S3. Theoretical and observed masses (m/z) of metal-free and metallated peptides. The observed masses are shown in parentheses. Observed masses corresponding to metal-free peptides are highlighted in blue; observed masses corresponding to metal-bound peptides are highlighted in red.

Metal (M)	Theoretical m/z $[P+2H]^{2+}$ (observed)	Theoretical m/z $[P+3H]^{3+}$ (observed)	Theoretical m/z $[P+4H]^{4+}$ (observed)	Theoretical m/z $[P+M+H]^{3+}$ (observed)	Theoretical m/z $[P+M+2H]^{4+}$ (observed)	Theoretical m/z $[P+M+2H+2MeOH]^{4+}$ (observed)
			P1			
none	1023.000 (1023.33)	682.335 (682.60)	512.003 (512.28)	--	--	--
Ni^{II}	1023.000	682.335	512.003	700.975 (701.57)	525.983 (526.45)	542.003 (541.45)
Cu^{II}	1023.000	682.335	512.003	702.640 (703.29)	527.232	543.252 (542.79)
			P4			
none	1065.531	710.690 (711.02)	533.269 (533.73)	--	--	--
Ni^{II}	1065.531	710.690	533.269	729.330 (729.57)	547.249 (547.70)	562.269
Co^{II}	1065.531	710.690	533.269 (533.31)	729.662 (729.77)	547.499 (547.84)	563.519
Cu^{II}	1065.531	710.690	533.269	730.995 (731.50)	548.498	564.518 (563.88)
Zn^{II}	1065.531	710.690 (710.60)	533.269 (533.44)	731.328	548.748 (549.36)	564.768
			P5			
none	1080.520	720.682 (721.04)	540.764 (541.07)	--	--	--
Ni^{II}	1080.520	720.682	540.764	739.323 (739.46)	554.744 (555.33)	570.764 (570.12)
Co^{II}	1080.520	720.682	540.764 (540.81)	739.655 (740.45)	554.993 (555.36)	571.013
Cu^{II}	1080.520	720.682	540.764	740.987 (741.25)	555.992	572.012 (571.27)
Zn^{II}	1080.520	720.682 (721.08)	540.764 (541.00)	741.320 (741.98)	556.243 (556.85)	572.263
			P6			
none	1044.994	696.998 (697.29)	523.001 (523.39)	--	--	--
Ni^{II}	1044.994	696.998	523.001	715.638 (716.32)	536.981 (537.49)	553.001 (552.56)
Cu^{II}	1044.994	696.998	523.001	717.303 (717.91)	538.229 (538.83)	554.249 (553.71)
			P7			
none	1036.007	518.507 (518.79)	415.007	--	--	--
Ni^{II}	1036.007	518.507	415.007	709.647 (709.87)	532.487 (532.98)	548.507 (547.97)
Co^{II}	1036.007	518.507 (518.72)	415.007	709.980 (710.34)	532.737 (533.05)	548.757 (548.03)
Cu^{II}	1036.007	518.507	415.007	711.312 (712.19)	533.736	549.756 (549.29)
Zn^{II}	1036.007	518.507 (518.79)	415.007	711.668	533.986 (534.51)	550.006 (549.23)

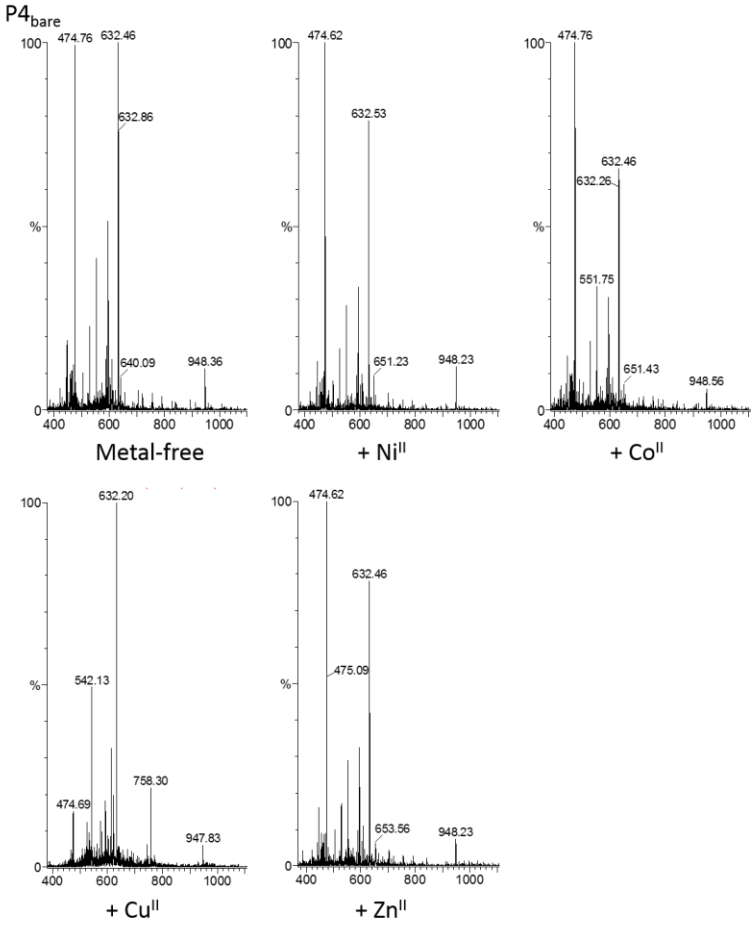

Figure S5. ESI spectra of $P4_{bare}$ after metal incubation. The only observed masses are those of the metal-free peptides.

Table S4. Theoretical and observed masses (m/z) of $P4_{bare}$, before and after incubation with metal. The observed masses are shown in parentheses. Observed masses corresponding to metal-free peptides are highlighted in blue; observed masses corresponding to metal-bound peptides were not observed.

Metal (M)	**Theoretical m/z $[P+2H]^{2+}$ (observed)**	**Theoretical m/z $[P+3H]^{3+}$ (observed)**	**Theoretical m/z $[P+4H]^{4+}$ (observed)**	**Theoretical m/z $[P+M+H]^{3+}$ (observed)**	**Theoretical m/z $[P+M+2H]^{4+}$ (observed)**	**Theoretical m/z $[P+M+2H+2MeOH]^{4+}$ (observed)**
			$P4_{bare}$			
none	947.490 (948.26)	631.996 (632.46)	474.249 (474.76)	--	--	--
Ni^{II}	947.490 (948.23)	631.996 (632.63)	474.249 (474.62)	650.636	488.229	504.249
Co^{II}	947.490 (948.56)	631.996 (632.46)	474.249 (474.76)	650.968	488.478	504.498
Cu^{II}	947.490 (947.83)	631.996 (632.20)	474.249	652.300	489.477	505.497
Zn^{II}	947.490 (948.23)	631.996 (632.46)	474.249 (474.62)	652.634	489.727	505.747

VI. Circular Dichroism Spectroscopy (CD)

Samples for circular dichroism spectroscopy (CD) analyses contained 15 µM peptide in 10 mM sodium borate buffer (NaB) at pH 7.1. The buffer had previously been treated using Chelex resin (BioRad) and all pipet tips were washed 3x with 10% analytical grade nitric acid (Fluka) before use. Peptide concentration was calculated by measuring the absorbance on a UV-vis spectrometer at 268 nm and calculating the corresponding concentration using an extinction coefficient of ε_{268} = 16,000 cm^{-1} M^{-1} for the metal-free peptide. A stock solution of approximately 15 µM peptide was first prepared, and then split into five 750 µl samples. A 3-6 fold excess of EDTA, $NiCl_2$, $CuSO_4$, $ZnCl_2$, or $CoCl_2$ was added to the sample to ensure the formation of a completely metal-free or metal-bound peptide, respectively, and each sample was incubated at room temperature for at least 1 h before analysis. For samples containing trifluoroethanol (TFE), peptides were prepared with a 3-fold excess of EDTA in 60% TFE, and no notable differences were measured for the apo or metal-bound peptides dissolved in TFE. CD measurements were recorded in a 1 cm square quartz cuvette (Starna Cells) on an Aviv 215 CD spectrometer. The CD spectrum of each sample was measured from 260-190 nm using a slit width of 1 nm, scanning at 1 nm intervals with a 1 s integration time. Measurements were taken at 25 and 4 °C with constant stirring. Each measurement was repeated 3-5 times, averaged and smoothed with a binomial function, and corrected for any background signal from the buffer solution (Fig. S4, Table S3) (See also Figure 2).

Table S5. Percent helicities for metal-peptide complexes by (top) comparison with a sample containing 60% TFE and (bottom) calculated using the ratio $[\theta]_{222}/[\theta]_{max}$. Here, $[\theta]_{222}$ is the molar ellipticity measured at 222 nm, and $[\theta]_{max}$ = (-44000 + 250T)*(1/(*k*-*n*)), where *k* is a constant and equal to 4, and *n* is the number of amide bonds and equal to 21.

Peptide	EDTA	Ni^{II}	Co^{II}	Cu^{II}	Zn^{II}
Percent helicity, vs. TFE (25 °C)					
P1	30.1	77.3	68.5	32.3	62.0
P2	49.8	53.6	52.9	57.5	48.6
P3	65.0	90.1	92.3	54.8	89.3
P4	56.9	82.1	73.9	52.7	73.3
P5	46.5	74.1	69.1	56.1	72.2
P6	33.0	57.1	50.8	43.3	48.7
P7	36.1	48.0	44.9	25.6	43.2
Percent helicity, vs. TFE (4 °C)					
P1	42.8	81.8	78.3	54.2	73.8
P2	75.2	76.7	75.5	77.9	74.5
P3	80.6	93.5	95.0	68.7	93.3
P4	76.1	93.3	88.9	57.9	89.7
P5	68.8	78.5	77.6	64.2	82.1
P6	47.4	72.7	68.7	69.9	69.6
P7	46.7	60.8	58.9	34.4	54.8
Percent helicity, calculated (25 °C)					
P1	16.7	42.9	38.0	17.9	34.3
P2	21.8	23.4	23.1	25.1	21.2
P3	34.3	48.0	48.8	29.0	47.2
P4	30.6	44.2	39.8	28.4	39.4

P5	28.4	45.3	42.2	34.2	44.0
P6	16.2	28.0	25.0	21.3	24.0
P7	15.1	20.1	18.8	10.7	18.1
			Percent helicity, calculated (4 °C)		
P1	24.7	47.1	45.1	31.2	42.6
P2	31.6	32.2	31.7	32.7	31.3
P3	43.6	50.5	41.3	37.1	50.4
P4	42.6	52.2	49.7	32.3	50.2
P5	45.0	51.3	50.7	42.0	53.7
P6	26.2	40.2	38.0	38.6	38.4
P7	20.9	26.4	27.3	15.4	24.5

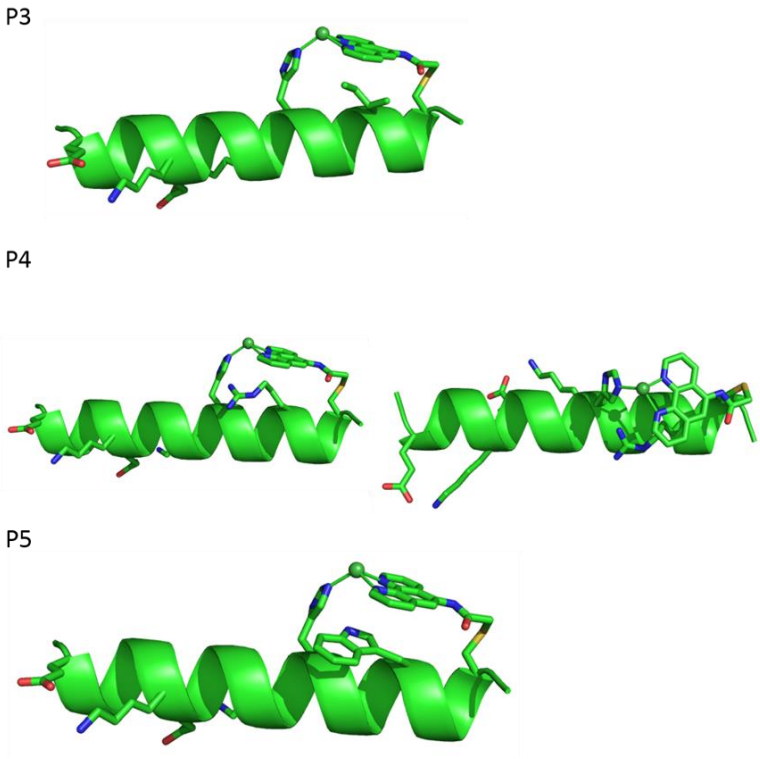

Figure S6. Models of P3, P4, and P5. The bulky, hydrophobic amino acids placed at position i+4 are accommodated in the hydrophobic “pocket” formed when metal is coordinated to the HCM.

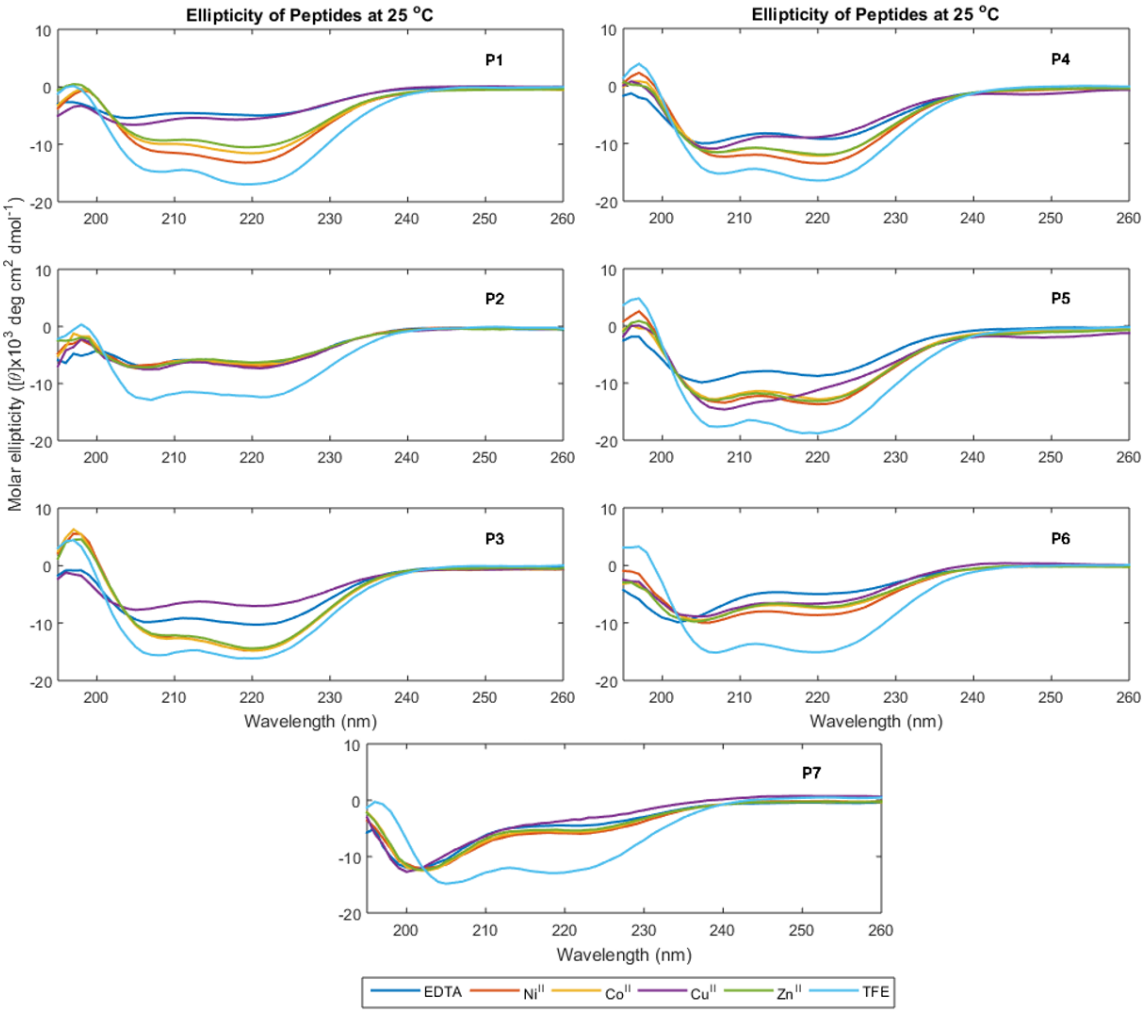

Figure S7. CD spectra of peptides at 25 °C. Samples were prepared with approximately 15 µM of peptide with an excess of either M^{II} or EDTA. For each graph, EDTA = blue, Ni^{II} = red, Co^{II} = yellow, Cu^{II} = purple, Zn^{II} = green, and 60% TFE = cyan. The samples in 60% TFE were metal free; no further induction of helicity was observed upon the addition of metal.

VII. Density Functional Theory (DFT) Calculations

Computational details. Density Functional Theory calculations were carried out using the ORCA program package.[7] Geometry optimizations were performed using the OLYP functional[8] and the all-electron Ahlrichs triple-zeta basis set def2-TZVP (standard)[9] and def2-TZVP/J (auxiliary).[10] The Conductor-Like Screening Model (COSMO)[11] was utilized to simulate the presence of a polarizable continuum (aqueous solvent). Optimized structures were visualized using ChemCraft.[12] The initial guess for each optimization was an octahedral six-coordinate Cu(II) or Ni(II) complex bearing three aqua ligands in a *fac* geometry. The histidine binding site was modeled using 4-methylimidazole, while the bidentate donor of the HCM was modeled with 1,10 phenanthroline or 8-hydroxyquinoline containing 5-formamyl substitution. In the case of 8-hydroxyquinoline, optimizations were run both with the O-donor protonated (neutral phenol donor) and deprotonated (anionic phenolate donor).

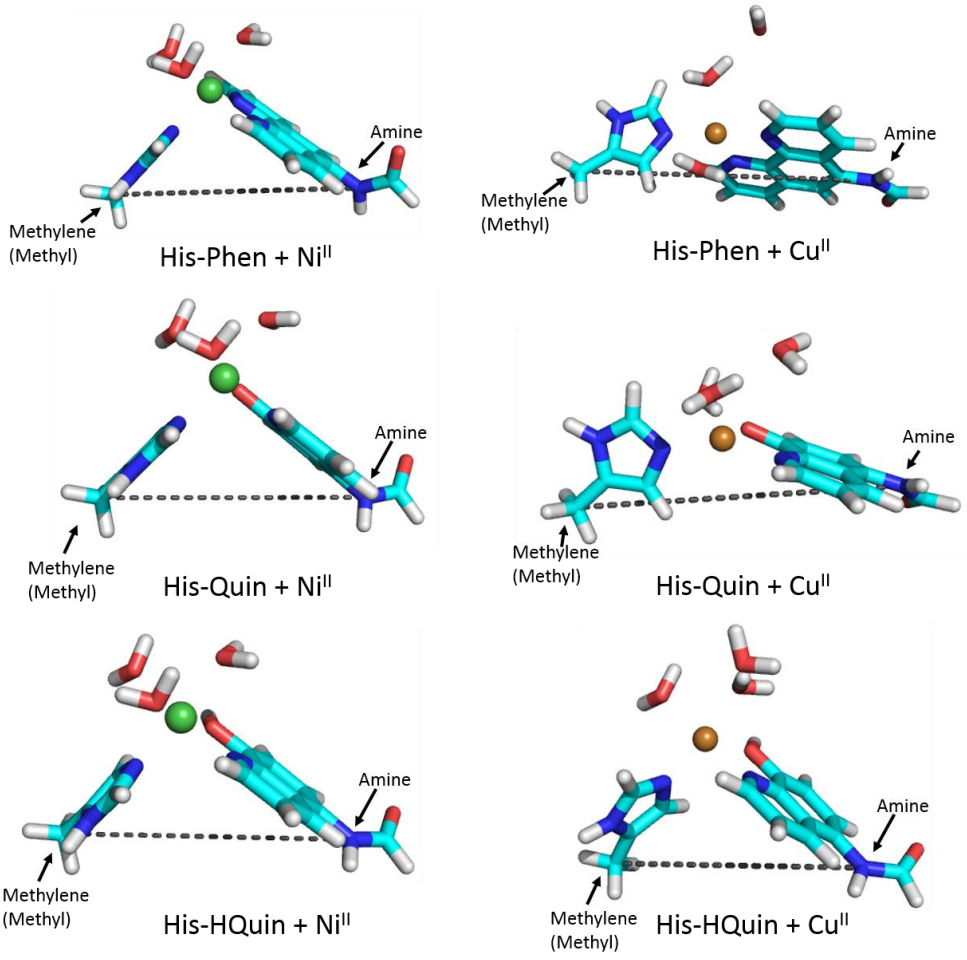

Structure	Number of coordinated water molecules	Methylene-to-amine distance
His-Quin protein crystal structure + Ni^{II}	N/A	9.5 Å
His-Phen + Ni^{II}	3	9.3 Å
His-Phen + Cu^{II}	2	11.6 Å
His-Quin + Ni^{II}	3	8.9 Å
His-Quin + Cu^{II}	1	11.0 Å
His-HQuin + Ni^{II}	3	9.1 Å
His-HQuin + Cu^{II}	2	8.5 Å

Figure S8. Lowest energy His-Quin or His-Phen HCMs when bound to Ni^{II} or Cu^{II} as calculated using DFT. The measured distances between the His methylene group and the Phen or Quin amine group is also shown, and indicated with dashed lines.

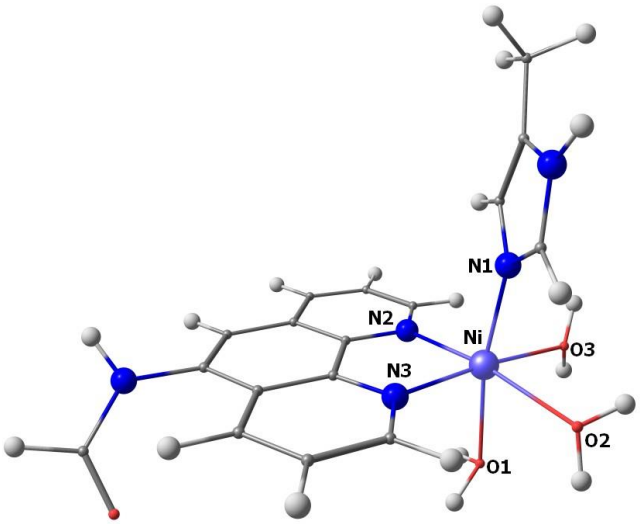

Figure S9. Optimized structure of Ni(Phen)(Im)$(H_2O)_3$. Selected bond distances (Å) and angles (˚): Ni-N1 = 2.08; Ni-N2 = 2.07; Ni-N3 = 2.07; Ni-O1 = 2.26; Ni-O2 = 2.22; Ni-O3 = 2.22; N1-Ni-N2 = 97.4; N1-Ni-N3 = 96.3.

Input for geometry optimization of Ni(Phen)(Im)$(H_2O)_3$

```
%pal nprocs 8 end
! UKS OLYP Opt RI def2-TZVP def2-TZVP/J TightSCF SlowConv KeepDens NormalPrint
! COSMO(Water)
%SCF
 MaxIter 1000
end
%geom
 MaxIter 1000
end
%output
Print[ P_Basis ] 2
Print[ P_MOs ] 1
end

* xyz 2 3
Ni      8.86859800      4.70157900      8.88575100
H      10.42185000      8.50128300      6.10285100
C      12.05047800      7.55962900      6.69279300
H      12.63628900      8.07885900      6.54100400
C      12.45530700      6.49476900      7.46895000
C      13.82422300      6.08114600      7.69585100
H      14.66360200      6.67077900      7.13564100
C      14.11819400      5.00924500      8.42193400
N      15.40633507      4.34690045      8.48895854
C      13.09055800      4.21367900      9.03534900
C       7.19364048      2.70994295      7.34881778
N       7.16267746      1.98213424      6.14960084
```

C	9.79449800	7.04392000	7.14033500
C	8.44315734	2.27580075	5.47583040
H	12.57717600	1.61929200	10.92253800
C	11.01610800	2.90768500	10.22462200
H	10.13075400	2.41133700	10.75040600
N	8.30031239	3.36904440	7.53600918
N	10.71630100	3.94614400	9.47037300
C	11.78757400	4.59562100	8.88825400
C	11.45135300	5.72208500	8.06828200
H	8.85676900	7.30441500	7.02610300
C	9.25441652	2.90947212	6.48078240
C	13.31776900	3.07841500	9.81620100
H	14.06430100	2.88656400	10.03058300
C	10.76522600	7.85708600	6.54569900
N	10.12373000	5.99666100	7.88989100
C	12.31547300	2.43245800	10.40927300
H	6.35486763	1.66650664	5.84876286
O	9.07962039	5.69615852	10.49083079
H	9.11516101	6.63303308	10.28442602
H	9.87993392	5.43386788	10.97208112
O	8.05765467	3.46376376	10.06103263
H	7.56147455	3.90782594	10.65658100
H	8.36409632	2.93959360	10.76547508
O	7.31986023	5.77525235	8.51827740
H	7.06173727	5.66111196	7.60070206
H	7.70940747	6.61997026	8.65357194
H	15.55813834	3.60473587	7.97612221
C	15.98776720	4.16681107	9.69395003
C	8.88515955	1.71367991	4.13454213
H	9.85339608	2.04086087	3.78544238
H	8.16668259	1.79565106	3.33237532
H	9.01803515	0.64515288	4.21817264
H	10.32877124	3.01542434	6.45018646
H	6.40788597	2.76013035	8.08805460
O	15.96836022	4.99378863	10.64438755
H	16.52852443	3.26044741	9.92304946

*

Optimized coordinates for Ni(Phen)(Im)(H_2O)$_3$

Ni	8.96077458190854	4.69875622875788	8.89032431982578
H	10.79047693030219	8.45913202740471	5.71733660687756
C	12.37322242415019	7.26466228971567	6.56534199519101
H	13.18002822219976	7.79537647550037	6.06653554550955
C	12.66918506001666	6.18809343596440	7.43265816336953
C	13.99856257158501	5.75898698948621	7.72587817917414
H	14.82881375204681	6.28217131969160	7.25938646669484
C	14.24748077315926	4.72418641227303	8.59057360821889
N	15.59176068860525	4.33035088407847	8.82241838968718
C	13.15605117084364	4.01119680575439	9.21463229110986

C	8.29371236636548	2.04838307373049	7.52885280051154
N	8.07706417457099	1.47055258559914	6.32968813282778
C	10.03797839927396	6.92247174818622	7.02711607887004
C	8.21139104308171	2.41868397774640	5.33772793686619
H	12.28768037500442	1.41090334299132	11.24360927665929
C	10.92245348143156	2.79448252161190	10.31398561798683
H	10.03295254374904	2.34507793154634	10.74439528544157
N	8.56577543448835	3.34093360153180	7.37092394172915
N	10.74373515039566	3.83731237021752	9.50693881918817
C	11.82852521607731	4.43904403529585	8.95011065242334
C	11.57993422656545	5.53315985578339	8.05570285652287
H	8.99630024011402	7.19528955364044	6.88522561818935
C	8.51878148973406	3.58012005168058	6.00853557615179
C	13.31082000818740	2.88206385759628	10.04953942948682
H	14.29698533870498	2.48330125831464	10.25563983391181
C	11.05646133703613	7.63317364965488	6.37009026557791
N	10.28871265609804	5.89773298043502	7.84049056002626
C	12.19603825735662	2.27890718452063	10.59790818066257
H	7.84608198634319	0.49492518357427	6.19313207219226
O	9.00550402808453	6.15814942270219	10.61763098078957
H	9.26594615116124	7.05996014575552	10.37699533188854
H	9.62289861013256	5.92248341393858	11.32630901823728
O	7.68606873768216	3.51407785282151	10.27655592703620
H	6.77562522317247	3.56576693592932	9.94702200043684
H	7.63478827272829	3.92662058202579	11.15196376396979
O	7.05660452927708	5.73261477482288	8.41606516687980
H	6.70953025857540	5.73805030463276	7.51311412389438
H	6.88253173456070	6.62017582229549	8.76045474087928
H	16.17372435662962	4.20811084453848	8.00190520072624
C	16.26131699488339	4.39709817769769	10.01255610848937
C	8.03470123657496	2.11775120894319	3.89008657090857
H	8.20359069919165	3.01986401021367	3.29708264776155
H	7.02098395369513	1.75606041319480	3.67797404106567
H	8.73964200467375	1.34820694694477	3.55275833748949
H	8.70812218428189	4.55551023411479	5.58574900802554
H	8.24283311149621	1.50881708462619	8.46251249500416
O	15.77545872127891	4.70461141802174	11.09453719039684
H	17.32559378252439	4.12635106449680	9.88473566523693

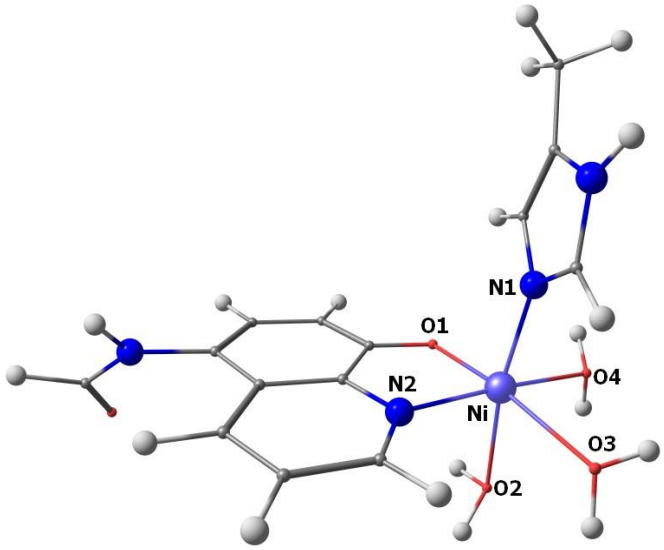

Figure S10. Optimized structure of Ni(Quin)(Im)$(H_2O)_3$. Selected bond distances (Å) and angles (˚): Ni-N1 = 2.07; Ni-N2 = 2.05; Ni-O1 = 2.02; Ni-O2 = 2.33; Ni-O3 = 2.26; Ni-O4 = 2.24; N1-Ni-N2 = 96.9; N1-Ni-O1 = 98.0.

Input for geometry optimization of Ni(Quin)(Im)$(H_2O)_3$

```
%pal nprocs 8 end
! UKS OLYP Opt RI def2-TZVP def2-TZVP/J TightSCF SlowConv KeepDens NormalPrint
! COSMO(Water)
%SCF
 MaxIter 1000
end
%geom
 MaxIter 1000
end
%output
Print[ P_Basis ] 2
Print[ P_MOs ] 1
end

* xyz 1 3
Ni      8.86859800      4.70157900      8.88575100
H       8.16668259      1.79565106      3.33237532
H       9.01803515      0.64515288      4.21817264
H      10.32877124      3.01542434      6.45018646
C      12.45530700      6.49476900      7.46895000
C      13.82422300      6.08114600      7.69585100
H      14.66360200      6.67077900      7.13564100
C      14.11819400      5.00924500      8.42193400
N      15.40633507      4.34690045      8.48895854
C      13.09055800      4.21367900      9.03534900
C       7.19364048      2.70994295      7.34881778
```

N	7.16267746	1.98213424	6.14960084
H	6.40788597	2.76013035	8.08805460
C	8.44315734	2.27580075	5.47583040
H	12.57717600	1.61929200	10.92253800
C	11.01610800	2.90768500	10.22462200
H	10.13075400	2.41133700	10.75040600
N	8.30031239	3.36904440	7.53600918
N	10.71630100	3.94614400	9.47037300
C	11.78757400	4.59562100	8.88825400
C	11.45135300	5.72208500	8.06828200
O	15.96836022	4.99378863	10.64438755
C	9.25441652	2.90947212	6.48078240
C	13.31776900	3.07841500	9.81620100
H	14.06430100	2.88656400	10.03058300
H	16.52852443	3.26044741	9.92304946
O	10.12373000	5.99666100	7.88989100
C	12.31547300	2.43245800	10.40927300
H	6.35486763	1.66650664	5.84876286
O	9.07962039	5.69615852	10.49083079
H	9.11516101	6.63303308	10.28442602
H	9.87993392	5.43386788	10.97208112
O	8.05765467	3.46376376	10.06103263
H	7.56147455	3.90782594	10.65658100
H	8.36409632	2.93959360	10.76547508
O	7.31986023	5.77525235	8.51827740
H	7.06173727	5.66111196	7.60070206
H	7.70940747	6.61997026	8.65357194
H	15.55813834	3.60473587	7.97612221
C	15.98776720	4.16681107	9.69395003
C	8.88515955	1.71367991	4.13454213
H	9.85339608	2.04086087	3.78544238
H	12.19095424	7.35404620	6.87048503

*

Optimized coordinates for Ni(Quin)(Im)(H_2O)$_3$

Ni	8.95933706889709	4.63033671395799	8.90332110432970
H	7.38404157221746	1.89191121743507	3.47324041303057
H	9.03485201297297	1.26363698012963	3.59969575799445
H	9.15413537590721	4.46323870697715	5.65124202202918
C	12.61268237776886	6.04910421771797	7.53070271784077
C	13.91620363120199	5.59083338528888	7.77610093811742
H	14.74473316049963	6.08361323486691	7.27443265635253
C	14.18430232436889	4.52384019610940	8.62396604670762
N	15.51753449905711	4.06624760120136	8.83137328350777
C	13.09935460821547	3.86628250841202	9.27239104294229
C	8.09468155560620	2.06249212425869	7.47378527065306
N	7.97619473101217	1.50537595318264	6.24953378806134
H	7.83258725351572	1.54775913542650	8.38626101718167
C	8.39284084683184	2.41320865054775	5.29790466761052

H	12.18959901338438	1.39176591079939	11.45034011799866
C	10.83535351135757	2.71836905782419	10.41597421189224
H	9.93636340327950	2.28446280093693	10.84478290926688
N	8.56999749951624	3.29885102326877	7.36972075627960
N	10.67771452592099	3.73460799017159	9.57639092061972
C	11.76927357404055	4.32004363545641	9.00343192490476
C	11.49894628047215	5.43236231587096	8.12299804933537
O	16.53083864888145	5.95710085616456	9.69589758700540
C	8.76108641466029	3.52673785127000	6.01895776552208
C	13.23037770076340	2.78530535072099	10.18229895552956
H	14.21531461075751	2.40772367977304	10.44151690704773
H	17.48264689069083	4.17373243534938	9.36071879190015
O	10.26476037053945	5.81151948397198	7.92225915448970
C	12.10845588123187	2.21778452258146	10.74927653331135
H	7.63623104455600	0.56972614392791	6.07043817448427
O	9.01992770392365	6.23616696793671	10.58823061479026
H	9.59577097443803	6.92476082739482	10.22293586167906
H	9.46216649006515	5.97461595805092	11.40931914022795
O	7.49989609047233	3.57246071754922	10.26103642657051
H	6.60614746904007	3.71630050117124	9.91513396321387
H	7.46706748164685	3.96187093688265	11.14712318275340
O	7.16997760828288	5.83496777761940	8.28986262451579
H	7.27152400884146	6.19782389522368	7.39747814295411
H	7.07693753667782	6.61613530773696	8.85517897362182
H	15.72729248976042	3.10209311080689	8.60212391005158
C	16.55926030930744	4.78473783093930	9.32534048475240
C	8.39314027631183	2.12120987561524	3.83701130183785
H	8.76499147367056	2.98668068779097	3.28272361871878
H	12.45450842943671	6.89076841168248	6.85995511836615

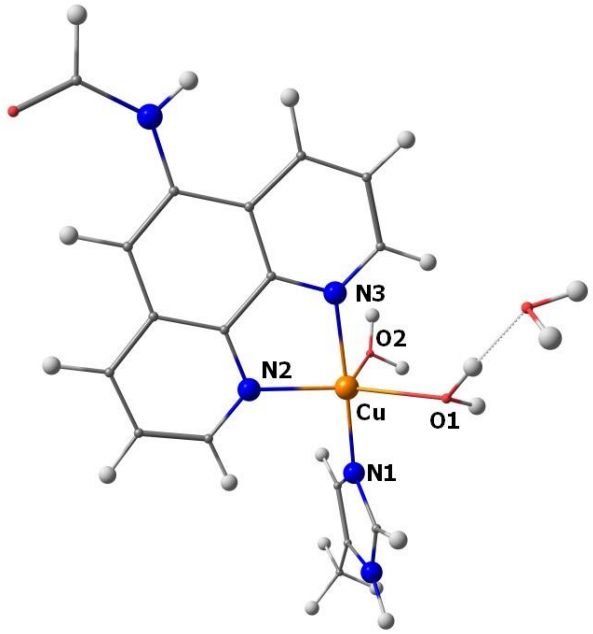

Figure S11. Optimized structure of Cu(Phen)(Im)(H_2O)$_3$. Selected bond distances (Å) and angles (˚): Cu-N1 = 2.00; Cu-N2 = 2.06; Cu-N3 = 2.03; Cu-O1 = 2.15; Cu-O2 = 2.47; N1-Cu-N2 = 97.3; N1-Cu-N3 = 176.1.

Input for geometry optimization of Cu(Phen)(Im)(H_2O)$_3$

```
%pal nprocs 8 end
! UKS OLYP Opt RI def2-TZVP def2-TZVP/J TightSCF SlowConv KeepDens NormalPrint
! COSMO(Water)
%SCF
 MaxIter 1000
end
%geom
 MaxIter 1000
end
%output
Print[ P_Basis ] 2
Print[ P_MOs ] 1
end

* xyz 2 2
Cu      8.86859800      4.70157900      8.88575100
H      10.42185000      8.50128300      6.10285100
C      12.05047800      7.55962900      6.69279300
H      12.63628900      8.07885900      6.54100400
C      12.45530700      6.49476900      7.46895000
C      13.82422300      6.08114600      7.69585100
H      14.66360200      6.67077900      7.13564100
```

C	14.11819400	5.00924500	8.42193400
N	15.40633507	4.34690045	8.48895854
C	13.09055800	4.21367900	9.03534900
C	7.19364048	2.70994295	7.34881778
N	7.16267746	1.98213424	6.14960084
C	9.79449800	7.04392000	7.14033500
C	8.44315734	2.27580075	5.47583040
H	12.57717600	1.61929200	10.92253800
C	11.01610800	2.90768500	10.22462200
H	10.13075400	2.41133700	10.75040600
N	8.30031239	3.36904440	7.53600918
N	10.71630100	3.94614400	9.47037300
C	11.78757400	4.59562100	8.88825400
C	11.45135300	5.72208500	8.06828200
H	8.85676900	7.30441500	7.02610300
C	9.25441652	2.90947212	6.48078240
C	13.31776900	3.07841500	9.81620100
H	14.06430100	2.88656400	10.03058300
C	10.76522600	7.85708600	6.54569900
N	10.12373000	5.99666100	7.88989100
C	12.31547300	2.43245800	10.40927300
H	6.35486763	1.66650664	5.84876286
O	9.07962039	5.69615852	10.49083079
H	9.11516101	6.63303308	10.28442602
H	9.87993392	5.43386788	10.97208112
O	8.05765467	3.46376376	10.06103263
H	7.56147455	3.90782594	10.65658100
H	8.36409632	2.93959360	10.76547508
O	7.31986023	5.77525235	8.51827740
H	7.06173727	5.66111196	7.60070206
H	7.70940747	6.61997026	8.65357194
H	15.55813834	3.60473587	7.97612221
C	15.98776720	4.16681107	9.69395003
C	8.88515955	1.71367991	4.13454213
H	9.85339608	2.04086087	3.78544238
H	8.16668259	1.79565106	3.33237532
H	9.01803515	0.64515288	4.21817264
H	10.32877124	3.01542434	6.45018646
H	6.40788597	2.76013035	8.08805460
O	15.96836022	4.99378863	10.64438755
H	16.52852443	3.26044741	9.92304946

*

Optimized coordinates of Cu(Phen)(Im)(H_2O)$_3$

Cu	9.52083624466020	3.88651325991543	8.22618405337724
H	11.80312478147636	5.92070126313030	3.97659213228313
C	13.09401340528607	5.96199318565733	5.70221140468488
H	13.92896164362916	6.43444165966475	5.19076100556146
C	13.20517836510005	5.63014936831876	7.07379634766034

C	14.37609656675655	5.87129055160242	7.84864685940391
H	15.22682409068089	6.33326158313761	7.36611614818478
C	14.44847250165056	5.52120222526012	9.18037257844134
N	15.59197419584760	5.73167808717440	9.95432126165754
C	13.30225812955003	4.90340233537682	9.83108254892325
C	7.06253546454326	4.36555639691201	6.61168929911356
N	6.35976592093522	3.88638342696654	5.56874011562608
C	10.85843945684969	5.06285054244476	5.71066557165071
C	6.97916721742102	2.75502016756143	5.07723260868584
H	12.05198396750664	3.61131028832578	12.73441170205761
C	11.00223103630131	3.72160036576968	10.85809847960430
H	10.09567581006741	3.25632203830965	11.22975343433849
N	8.12243686207116	3.58968350545572	6.82918924290199
N	11.01747484877280	4.09448540153770	9.58146463940853
C	12.13586013871244	4.66533664712535	9.06004286745207
C	12.08356026757495	5.01873899193648	7.67793161791558
H	9.93282693628083	4.82941234637081	5.19632072448997
C	8.08510235213846	2.58597253890373	5.87690174523972
C	13.24772046822437	4.51580884734601	11.18880880255247
H	14.08236262963886	4.67453798264397	11.86428144004767
C	11.92259090115695	5.67915642422634	5.02825841462623
N	10.94106376090891	4.74164389867768	6.99901404314972
C	12.10733511711785	3.92098720498284	11.69587484957705
H	5.50700703078098	4.29852228803307	5.21278180561185
O	7.95195026100492	4.31240177469995	9.63128671667659
H	8.07870478012132	4.76626542412524	10.50576909668075
H	7.32936434979889	3.58996170952385	9.79166183291547
O	9.71078274799533	1.43876910052498	8.49852068816111
H	8.88635648387156	0.96397382201422	8.67816574489921
H	10.32665670556383	1.09559711088979	9.16180167458709
O	8.24308494356907	5.68326320199513	11.98467002068509
H	7.80964593922578	5.22541388814153	12.72020652472023
H	7.75653641134828	6.51792350402666	11.91187156027714
H	15.59558451234766	5.32500333504917	10.87850111416905
C	16.74778879359896	6.41709885440919	9.66646521540537
C	6.45362617267008	1.96905823419423	3.92722422462735
H	7.11143774136905	1.12090818502106	3.72424566447337
H	6.39301267697166	2.58330364112451	3.02063286409278
H	5.44867729604071	1.58267453091686	4.13432823365280
H	8.83642097030193	1.81133553650003	5.83115007141018
H	6.78541249385636	5.24807971588670	7.16901451442591
O	17.01334963926179	7.00585294683077	8.62766651606140
H	17.44193145944213	6.37486495135861	10.52597879785174

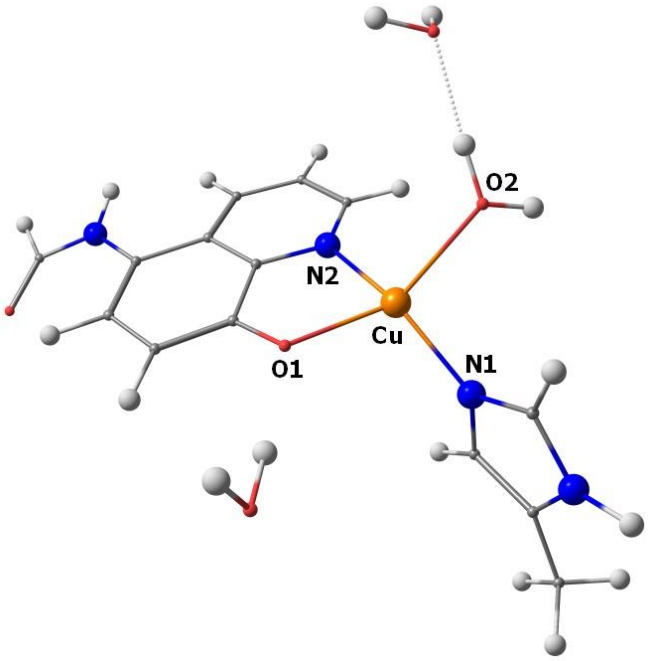

Figure S12. Optimized structure of Cu(Quin)(Im)$(H_2O)_3$. Selected bond distances (Å) and angles (˚): Cu-N1 = 1.98; Cu-N2 = 2.03; Cu-O1 = 2.06; Cu-O2 = 2.20; N1-Cu-N2 = 151.4; N1-Cu-O1 = 103.4.

Input for geometry optimization of Cu(Quin)(Im)$(H_2O)_3$

```
%pal nprocs 8 end
! UKS OLYP Opt RI def2-TZVP def2-TZVP/J TightSCF SlowConv KeepDens NormalPrint
! COSMO(Water)
%SCF
 MaxIter 1000
end
%geom
 MaxIter 1000
end
%output
Print[ P_Basis ] 2
Print[ P_MOs ] 1
end

* xyz 1 2
Cu      8.86859800      4.70157900      8.88575100
H       8.16668259      1.79565106      3.33237532
H       9.01803515      0.64515288      4.21817264
H      10.32877124      3.01542434      6.45018646
C      12.45530700      6.49476900      7.46895000
C      13.82422300      6.08114600      7.69585100
H      14.66360200      6.67077900      7.13564100
C      14.11819400      5.00924500      8.42193400
N      15.40633507      4.34690045      8.48895854
C      13.09055800      4.21367900      9.03534900
```

C	7.19364048	2.70994295	7.34881778
N	7.16267746	1.98213424	6.14960084
H	6.40788597	2.76013035	8.08805460
C	8.44315734	2.27580075	5.47583040
H	12.57717600	1.61929200	10.92253800
C	11.01610800	2.90768500	10.22462200
H	10.13075400	2.41133700	10.75040600
N	8.30031239	3.36904440	7.53600918
N	10.71630100	3.94614400	9.47037300
C	11.78757400	4.59562100	8.88825400
C	11.45135300	5.72208500	8.06828200
O	15.96836022	4.99378863	10.64438755
C	9.25441652	2.90947212	6.48078240
C	13.31776900	3.07841500	9.81620100
H	14.06430100	2.88656400	10.03058300
H	16.52852443	3.26044741	9.92304946
O	10.12373000	5.99666100	7.88989100
C	12.31547300	2.43245800	10.40927300
H	6.35486763	1.66650664	5.84876286
O	9.07962039	5.69615852	10.49083079
H	9.11516101	6.63303308	10.28442602
H	9.87993392	5.43386788	10.97208112
O	8.05765467	3.46376376	10.06103263
H	7.56147455	3.90782594	10.65658100
H	8.36409632	2.93959360	10.76547508
O	7.31986023	5.77525235	8.51827740
H	7.06173727	5.66111196	7.60070206
H	7.70940747	6.61997026	8.65357194
H	15.55813834	3.60473587	7.97612221
C	15.98776720	4.16681107	9.69395003
C	8.88515955	1.71367991	4.13454213
H	9.85339608	2.04086087	3.78544238
H	12.19095424	7.35404620	6.87048503

*

Optimized coordinates of Cu(Quin)(Im)(H_2O)$_3$

Cu	9.38381530670972	3.54019396521800	8.44406262800632
H	7.04387045934200	2.13384994029956	2.88630859976076
H	6.52497415205442	0.66855704787818	3.73662686976262
H	9.54409277718955	1.81712829149512	5.73600116009273
C	12.63949763267523	6.01001620402315	7.57160241066267
C	13.91197085233168	6.06787192855421	8.14207401632553
H	14.62373959943541	6.78669744201093	7.75683968220438
C	14.29064124536353	5.23411446355077	9.19957956300585
N	15.55641045571965	5.29639979786304	9.78885847283951
C	13.34836083773240	4.26553394109906	9.69919762373285
C	6.93159835758489	3.35536411012362	6.76042416412865
N	6.47504657661944	2.84739688839790	5.59782959196898
H	6.33082369533064	3.96019137892209	7.42477794841151

C	7.48333606316696	2.12893908462864	4.98768024928232
H	12.85842131825397	1.61709501954522	11.80155883455940
C	11.38180538426192	2.45878484110650	10.47356142788812
H	10.58916011341576	1.77685611785270	10.77012375674316
N	8.20026103317182	3.00038414108607	6.94416780871328
N	11.09203293886246	3.34995114146023	9.52609705369962
C	12.03923072170678	4.24667731125376	9.13899313793837
C	11.64273536448347	5.15367195801947	8.08206641796807
O	16.92296384718276	6.31488637761812	8.20963803885149
C	8.55461836781901	2.23856709739038	5.84369487791997
C	13.63340426582845	3.28065979212965	10.67442731239174
H	14.61966569860225	3.19697605947424	11.12102654407332
H	17.53689296072812	5.70351748278057	10.06479221299440
O	10.40954017355885	5.15997085336620	7.68510458752828
C	12.65407775521285	2.38307666991886	11.05936964939300
H	5.53831833477418	2.97827602377823	5.23907601043664
O	8.40374948458762	4.05300945992532	12.67421599658640
H	8.93727036707305	4.85712236664250	12.75139989654036
H	8.86248797655930	3.40729581148711	13.23077424730509
O	7.85650188195370	3.36016033871525	10.01158087964435
H	8.10659311318195	3.54893220668297	10.94603671528276
H	7.40747348293220	2.50350592776902	10.03394405036469
O	9.28631959631984	6.95462623193537	5.50324735870544
H	9.64364120546438	6.33713975766224	6.16450144694649
H	9.09082594351978	7.75195407300893	6.01442422967017
H	15.63914092061045	4.90402906057767	10.71717275574744
C	16.73635968258001	5.80881323175391	9.30960941387641
C	7.31286403624988	1.43020608242909	3.68344510417914
H	8.24572669243997	0.93649273640751	3.40000597553522
H	12.38878805740965	6.68367383415862	6.75648812833251

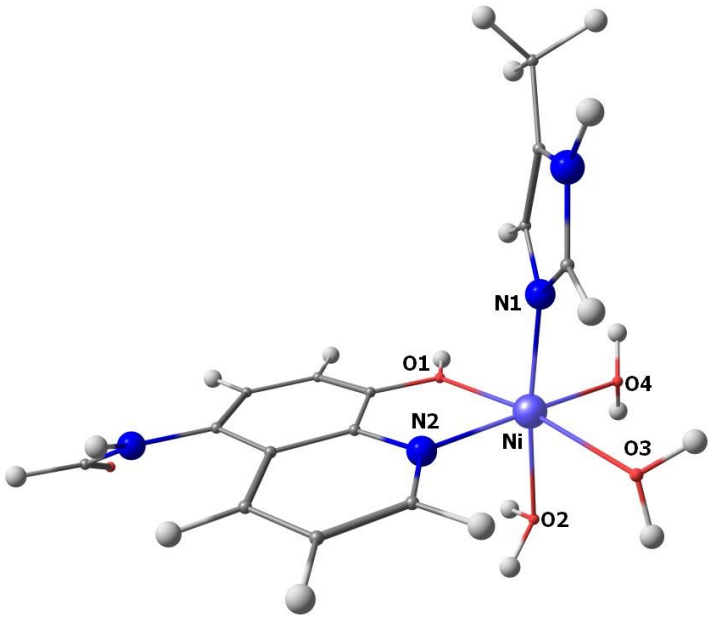

Figure S13. Optimized structure of Ni(QuinH)(Im)(H_2O)$_3$. Selected bond distances (Å) and angles (˚): Ni-N1 = 2.06; Ni-N2 = 2.07; Ni-O1 = 2.19; Ni-O2 = 2.22; Ni-O3 = 2.14; Ni-O4 = 2.17; N1-Ni-N2 = 96.1; N1-Ni-O1 = 95.2.

Input for geometry optimization of Ni(QuinH)(Im)(H_2O)$_3$

```
%pal nprocs 8 end
! UKS OLYP Opt RI def2-TZVP def2-TZVP/J TightSCF SlowConv KeepDens NormalPrint
! COSMO(Water)
%SCF
 MaxIter 1000
end
%geom
 MaxIter 1000
end
%output
Print[ P_Basis ] 2
Print[ P_MOs ] 1
end

* xyz 2 3
Ni      8.86859800      4.70157900      8.88575100
H       8.16668259      1.79565106      3.33237532
H       9.01803515      0.64515288      4.21817264
H      10.32877124      3.01542434      6.45018646
C      12.45530700      6.49476900      7.46895000
C      13.82422300      6.08114600      7.69585100
H      14.66360200      6.67077900      7.13564100
C      14.11819400      5.00924500      8.42193400
N      15.40633507      4.34690045      8.48895854
```

C	13.09055800	4.21367900	9.03534900
C	7.19364048	2.70994295	7.34881778
N	7.16267746	1.98213424	6.14960084
H	6.40788597	2.76013035	8.08805460
C	8.44315734	2.27580075	5.47583040
H	12.57717600	1.61929200	10.92253800
C	11.01610800	2.90768500	10.22462200
H	10.13075400	2.41133700	10.75040600
N	8.30031239	3.36904440	7.53600918
N	10.71630100	3.94614400	9.47037300
C	11.78757400	4.59562100	8.88825400
C	11.45135300	5.72208500	8.06828200
O	15.96836022	4.99378863	10.64438755
C	9.25441652	2.90947212	6.48078240
C	13.31776900	3.07841500	9.81620100
H	14.06430100	2.88656400	10.03058300
H	16.52852443	3.26044741	9.92304946
O	10.12373000	5.99666100	7.88989100
C	12.31547300	2.43245800	10.40927300
H	6.35486763	1.66650664	5.84876286
O	9.07962039	5.69615852	10.49083079
H	9.11516101	6.63303308	10.28442602
H	9.87993392	5.43386788	10.97208112
O	8.05765467	3.46376376	10.06103263
H	7.56147455	3.90782594	10.65658100
H	8.36409632	2.93959360	10.76547508
O	7.31986023	5.77525235	8.51827740
H	7.06173727	5.66111196	7.60070206
H	7.70940747	6.61997026	8.65357194
H	15.55813834	3.60473587	7.97612221
C	15.98776720	4.16681107	9.69395003
C	8.88515955	1.71367991	4.13454213
H	9.85339608	2.04086087	3.78544238
H	12.19095424	7.35404620	6.87048503
H	9.82247450	6.88698308	7.75179059

*

Optimized coordinates for Ni(QuinH)(Im)(H_2O)$_3$

Ni	8.85138217399647	4.62190387260639	8.94879135506840
H	7.26024139069849	1.88354505229415	3.53857783480102
H	8.98790259343612	1.49619268073616	3.50607273241460
H	8.79885168240263	4.62065381503358	5.66220321736476
C	12.72543193594150	6.08101770137129	7.58550174278085
C	14.01972624250773	5.60699787791547	7.87118344265672
H	14.86381607704952	6.08732413697905	7.39305539741322
C	14.22427682914948	4.53652306057521	8.72795869243794
N	15.51463686050079	4.03769108739661	8.99737132757719
C	13.09534479639866	3.90413893108765	9.34518335834137
C	8.28409646783349	2.02850109758722	7.46876547370814

N	8.14940581257135	1.50093824261506	6.23575953909260
H	8.18238069896119	1.44948968536608	8.37450761939005
C	8.33679091109850	2.49026368200382	5.29359103953462
H	12.08119266676060	1.47907005162610	11.52776720810064
C	10.78361511857401	2.79899670359594	10.42186217364949
H	9.86911111530380	2.37695111234917	10.82710537962268
N	8.55253333201597	3.32817622545690	7.37969086961580
N	10.65633163615670	3.80684382457086	9.56731212606834
C	11.78068605491558	4.37320451911572	9.02742362567272
C	11.62549416477413	5.47087205208566	8.14464931153783
O	16.84634887187958	5.93598959210728	8.98662731632555
C	8.58953529185851	3.62586453469989	6.02825255467393
C	13.18147180334795	2.84039093367558	10.27586707033463
H	14.14651894346316	2.45668245312662	10.59154526032232
H	17.52571181223086	4.03517409590961	9.33176784699048
O	10.33009640886207	5.85806456390170	7.90612007335164
C	12.03573159817540	2.29163480316844	10.80922228639668
H	7.94059254754525	0.52955221260753	6.04384209741907
O	8.91927453607427	6.11549489651810	10.59002188087857
H	9.28669949504728	6.97158382986095	10.32307203626079
H	9.44987920655294	5.86552582824841	11.36130578321361
O	7.56529007202874	3.49043225112262	10.24134504110181
H	6.67953102258962	3.42912507808956	9.85055093885318
H	7.41410149814111	3.93764946267882	11.08851469327708
O	7.11526187968755	5.76662813922268	8.33428746689691
H	6.93691490582860	5.86650364198125	7.38806898968047
H	7.01964898907808	6.65675901726445	8.70354000422615
H	15.59714810085809	3.04429211956778	9.16771198660034
C	16.69182595202821	4.72626362831647	9.10694835056931
C	8.25454987407592	2.24591853976880	3.82709527085807
H	8.44983191384896	3.17191312844152	3.28117151651594
H	12.59988806648390	6.92172616958434	6.90699751998196
H	10.28242187926719	6.63308523776948	7.32598798842254

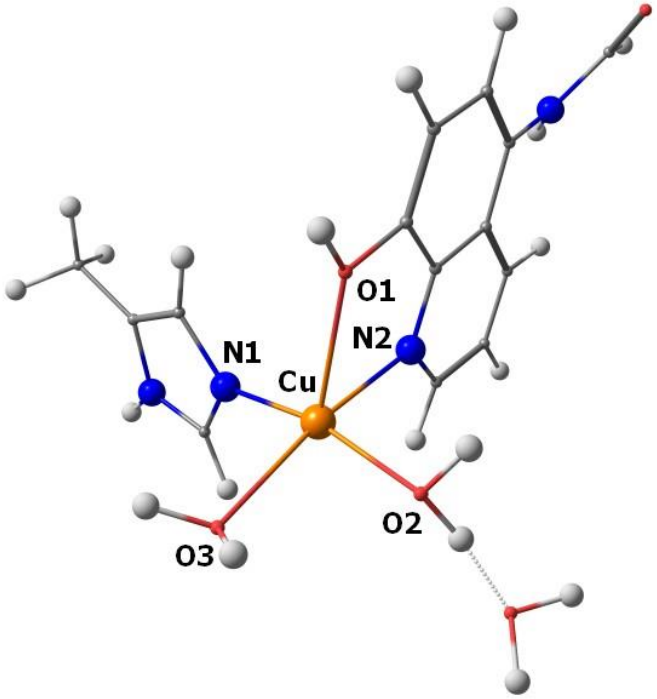

Figure S14. Optimized structure of Cu(QuinH)(Im)(H_2O)$_3$. Selected bond distances (Å) and angles (˚): Cu-N1 = 1.99; Cu-N2 = 2.05; Cu-O1 = 2.46; Cu-O2 = 2.08; Cu-O3 = 2.10; N1-Cu-N2 = 94.6; N1-Cu-O1 = 103.1.

Input for geometry optimization of Cu(QuinH)(Im)(H_2O)$_3$

```
%pal nprocs 8 end
! UKS OLYP Opt RI def2-TZVP def2-TZVP/J TightSCF SlowConv KeepDens NormalPrint
! COSMO(Water)
%SCF
 MaxIter 1000
end
%geom
 MaxIter 1000
end
%output
Print[ P_Basis ] 2
Print[ P_MOs ] 1
end

* xyz 2 2
Cu      8.86859800      4.70157900      8.88575100
H       8.16668259      1.79565106      3.33237532
H       9.01803515      0.64515288      4.21817264
H      10.32877124      3.01542434      6.45018646
C      12.45530700      6.49476900      7.46895000
C      13.82422300      6.08114600      7.69585100
```

H	14.66360200	6.67077900	7.13564100
C	14.11819400	5.00924500	8.42193400
N	15.40633507	4.34690045	8.48895854
C	13.09055800	4.21367900	9.03534900
C	7.19364048	2.70994295	7.34881778
N	7.16267746	1.98213424	6.14960084
H	6.40788597	2.76013035	8.08805460
C	8.44315734	2.27580075	5.47583040
H	12.57717600	1.61929200	10.92253800
C	11.01610800	2.90768500	10.22462200
H	10.13075400	2.41133700	10.75040600
N	8.30031239	3.36904440	7.53600918
N	10.71630100	3.94614400	9.47037300
C	11.78757400	4.59562100	8.88825400
C	11.45135300	5.72208500	8.06828200
O	15.96836022	4.99378863	10.64438755
C	9.25441652	2.90947212	6.48078240
C	13.31776900	3.07841500	9.81620100
H	14.06430100	2.88656400	10.03058300
H	16.52852443	3.26044741	9.92304946
O	10.12373000	5.99666100	7.88989100
C	12.31547300	2.43245800	10.40927300
H	6.35486763	1.66650664	5.84876286
O	9.07962039	5.69615852	10.49083079
H	9.11516101	6.63303308	10.28442602
H	9.87993392	5.43386788	10.97208112
O	8.05765467	3.46376376	10.06103263
H	7.56147455	3.90782594	10.65658100
H	8.36409632	2.93959360	10.76547508
O	7.31986023	5.77525235	8.51827740
H	7.06173727	5.66111196	7.60070206
H	7.70940747	6.61997026	8.65357194
H	15.55813834	3.60473587	7.97612221
C	15.98776720	4.16681107	9.69395003
C	8.88515955	1.71367991	4.13454213
H	9.85339608	2.04086087	3.78544238
H	12.19095424	7.35404620	6.87048503
H	9.82247450	6.88698308	7.75179059

*

Optimized coordinates of Cu(QuinH)(Im)(H_2O)$_3$

Cu	8.69495168752937	4.60325006426746	8.58680375065532
H	8.12291498140672	1.84285466816100	3.05129639814143
H	9.57199174587957	0.99402616100805	3.61719119216468
H	9.69220112800552	4.28249271283885	5.50671807839239
C	12.78753664483891	6.36078599783960	7.68915409413932
C	14.04017285716759	5.79866773197297	7.98141943831523
H	14.93119654419300	6.30687346753520	7.63499511384843
C	14.14969521755515	4.60656827393915	8.68286313292302

N	15.39977051181032	4.02716698536119	8.96729758963828
C	12.95875203901798	3.94129503221824	9.12506050077035
C	7.82575656260092	2.20159070111758	7.08195964950971
N	7.93242517410201	1.58642284131284	5.88981951832645
H	7.25719149965961	1.80778433730714	7.91251752365967
C	8.72200296913106	2.34430559157997	5.04940905393500
H	11.74885456362140	1.27926413514557	10.89837580481396
C	10.56194010752533	2.76229956657869	9.88133944748557
H	9.61264426809167	2.30194588446206	10.14148414322731
N	8.51622289755535	3.33988326910524	7.05684097895271
N	10.52088831126627	3.88886932685847	9.17829370051147
C	11.68117974098502	4.50642214286982	8.79702871141662
C	11.61897933202377	5.73197112665208	8.07456746697743
O	16.77410356114267	5.85758753541737	9.33732211372174
C	9.08243918600782	3.44011337337688	5.79884006874130
C	12.95767010403187	2.76116053063383	9.90610116685907
H	13.89082044825478	2.30791671910100	10.22390804284221
H	17.38461077452574	3.90488499786445	9.42478960686262
O	10.37578777471005	6.20700003847291	7.79251675577594
C	11.76951652638166	2.17836192952425	10.29107256476211
H	7.49804458437962	0.70196897801187	5.65928330808724
O	8.49012479062847	5.81035518747182	10.26871305708504
H	9.25386565167071	6.38327942826451	10.42868206952190
H	8.32718412425237	5.32331184352649	11.12849756508595
O	7.91117773998901	4.40266539422539	12.47904935526419
H	7.14918824955084	4.80136494291196	12.92559427354670
H	8.60725241909911	4.40463318842103	13.15306399521496
O	6.72865878680220	5.25831084919321	8.24598183210489
H	6.47500064528332	5.33215809895518	7.31326664610646
H	6.58186079551464	6.14014964778291	8.62354534690964
H	15.44610976854725	3.01667320977561	8.98614827866028
C	16.58483888565314	4.65013507848867	9.25782632418968
C	9.03599318550396	1.95031287875921	3.64847520016749
H	9.66581903309255	2.71048381947114	3.17930690843032
H	12.73834178975792	7.29400734247953	7.13302659945193
H	10.42584562125380	7.04397453973955	7.30475107280399

VIII. Thermal Denaturation as Monitored by CD

The thermal stability of the peptides was measured by monitoring the signal of each peptide at 222 nm as the temperature was increased from 4 °C to 90°C with a step size of either 2.5 or 5 °C. Each sample was incubated for at least 5 min after a stable temperature had been reached at each point, and the measurement was integrated for 10 s. In order to obtain the T_m, the data was smoothed using a binomial function, and the first derivative of the data was taken. This data was plotted, and was fit using the KaleidaGraph program as previously described (Fig. S5, Table S4, S5).[13]

Table S6. Calculated T_m for each of the peptide-metal combinations in degrees (°C). The signal at 222 nm was measured to observe peptide unfolding as the temperature was gradually increased. Wavelength scans from 260-190 nm were measured for each sample before and after the thermal unfolding experiment was performed in order to verify the reversibility of the unfolding.

Peptide	**EDTA**	**Ni^{II}**	**Co^{II}**	**Cu^{II}**	**Zn^{II}**
P1	16.3 ± 1.9	31.6 ± 2.9	26.5 ± 0.9	22.9 ± 0.7	23.8 ± 1.0
P2	23.6 ± 0.5	20.1 ± 1.1	22.1 ± 0.8	21.5 ± 0.9	21.6 ± 0.9
P3	23.8 ± 2.0	38.7 ± 2.4	37.2 ± 1.6	18.8 ± 1.7	33.7 ± 1.0
P4	20.2 ± 0.8	28.5 ± 0.7	24.6 ± 1.9	29.4 ± 2.1	23.0 ± 0.7
P5	15.8 ± 0.8	28.4 ± 1.2	26.0 ± 1.3	22.3 ± 1.6	24.3 ± 1.9
P6	16.2 ± 0.6	17.0 ± 1.0	17.8 ± 0.5	15.9 ± 0.5	16.6 ± 1.3
P7	10.5 ± 3.3	17.0 ± 1.4	16.7 ± 1.4	9.2 ± 1.5	8.5 ± 1.0

Table S7. Changes in the T_m (°C) for each peptide upon metal-binding. ΔT_ms were calculated by subtracting the T_m for each metal-free (EDTA) sample from metal-bound peptide.

Peptide	**Ni^{II}**	**Co^{II}**	**Cu^{II}**	**Zn^{II}**
P1	15.3	10.2	6.6	7.5
P2	-3.5	-1.5	-2.1	-2.0
P3	14.9	13.4	-5.0	9.9
P4	8.3	4.4	9.2	2.8
P5	12.6	10.2	6.5	7.5
P6	0.8	1.6	-0.3	0.4
P7	6.5	6.2	-1.3	-2.0

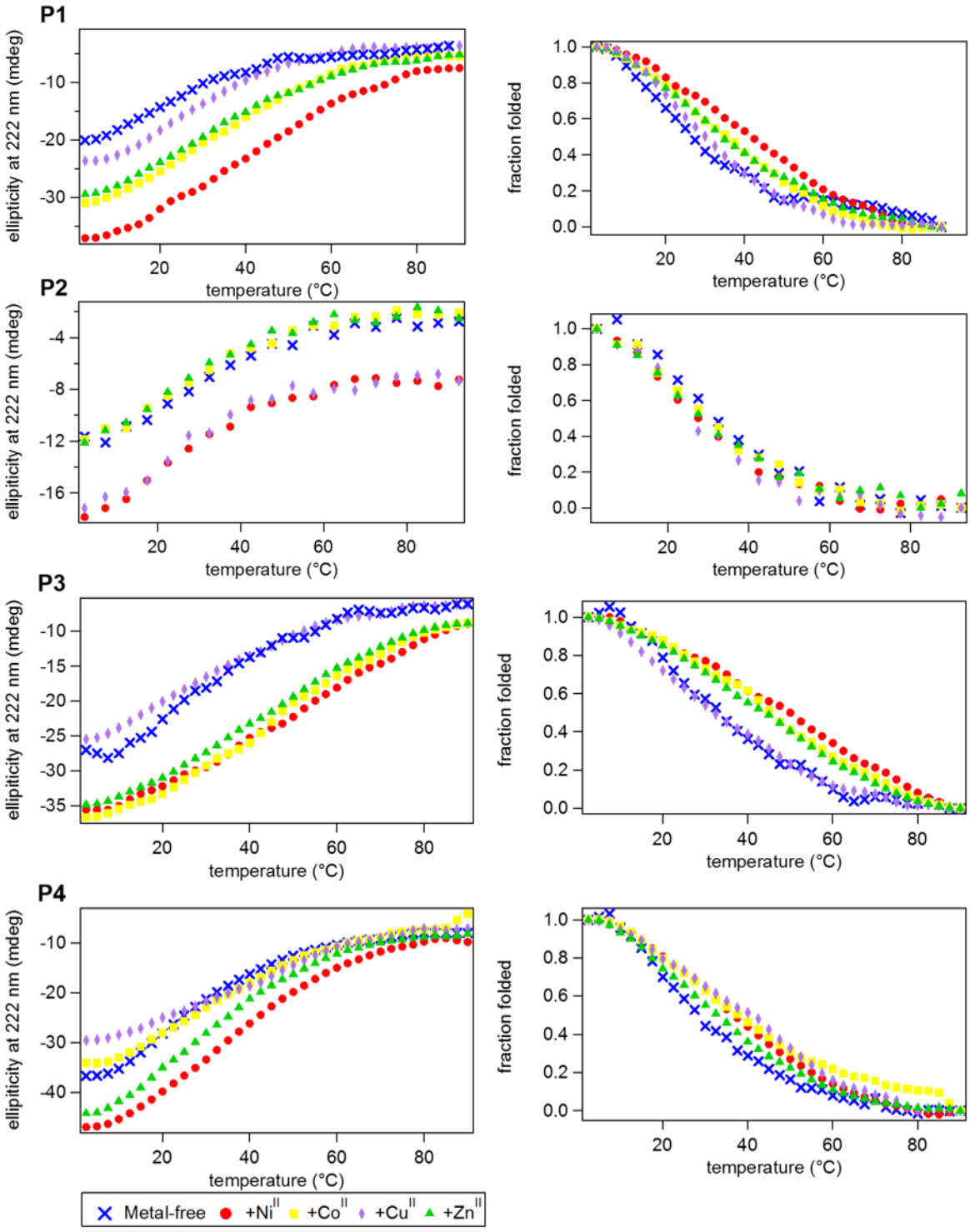

Figure S15. Thermal unfolding curves of peptides as monitored at 222 nm. The raw data is shown in the left panels, while the normalized unfolding curves are shown on the right.

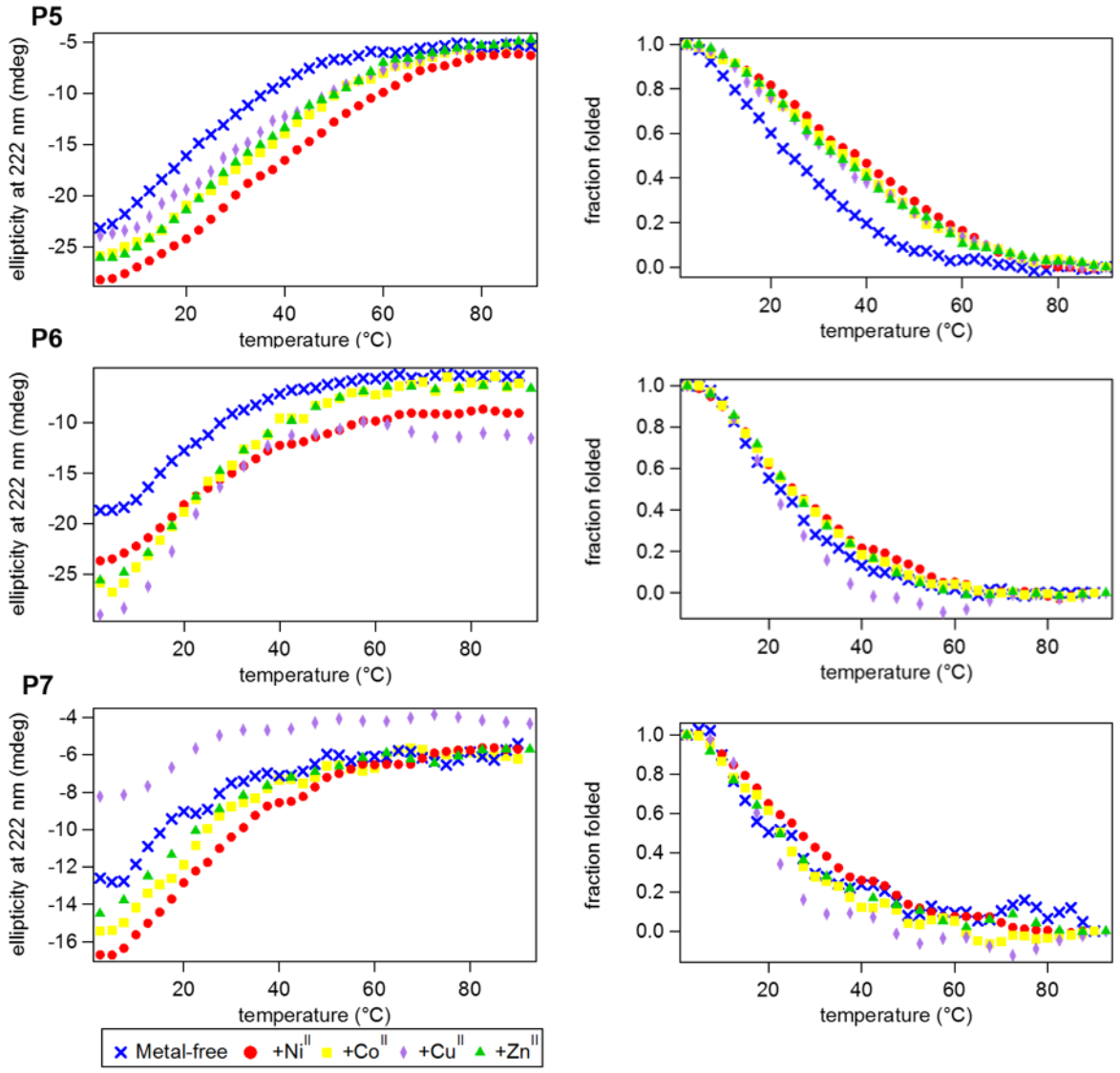

Figure S15, continued. Thermal unfolding curves of peptides as monitored at 222 nm. The raw data is shown in the left panels, while the normalized unfolding curves are shown on the right.

IX. Trypsin Digestion

Peptide samples were prepared at approximately 1.5 mM concentration with a three-fold excess of either EDTA for metal free samples or M^{II} in 100 mM tris(hydroxymethyl)aminomethane (Tris) buffer, pH 8 with 10 mM $CaCl_2$. Samples were equilibrated at 4 or 25 °C for 15 min before trypsin was added to a final concentration of 0.3 mg/mL. At each time point, 5 µL of the reaction solution as removed and added to 45 µL 1% trifluoroacetic acid. Each sample was run on the analytical HPLC as previously described, and the absorbance at 268 nm was monitored. In order to determine the fraction of intact peptide, the peaks corresponding to the intact peptide and cleaved peptide were integrated, where the fraction of intact peptide = intact peptide peak area/(intact peptide peak area + cleaved peptide peak area). The rate constants and peptide half-lives were calculated using the following equation for a first-order chemical reaction:

$$A(t) = A_0 \times e^{-kt}$$

where A(t) is the fraction of intact peptide, A_0 is the fraction of intact peptide at t = 0 (held at 1 for fitting), k is the rate of cleavage and t is time. Data was plotted as the fraction of peptide intact vs time (Fig. S6, S7) (See also Figure 3, Table 2).

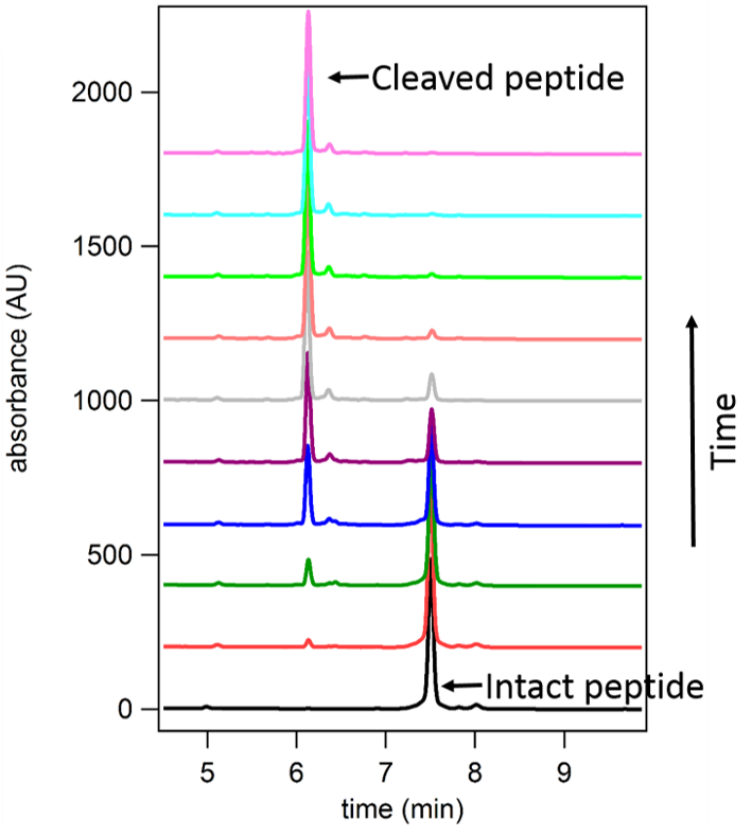

Figure S16. HPLC traces of the set of data collected for the metal-free, HCM-bound peptide during the tryptic digestion experiment. The intact peptide elutes at approximately 7.5 min; that peak disappears over time and a new peak at 6.0 min, corresponding to the cleaved peptide fragment, appears.

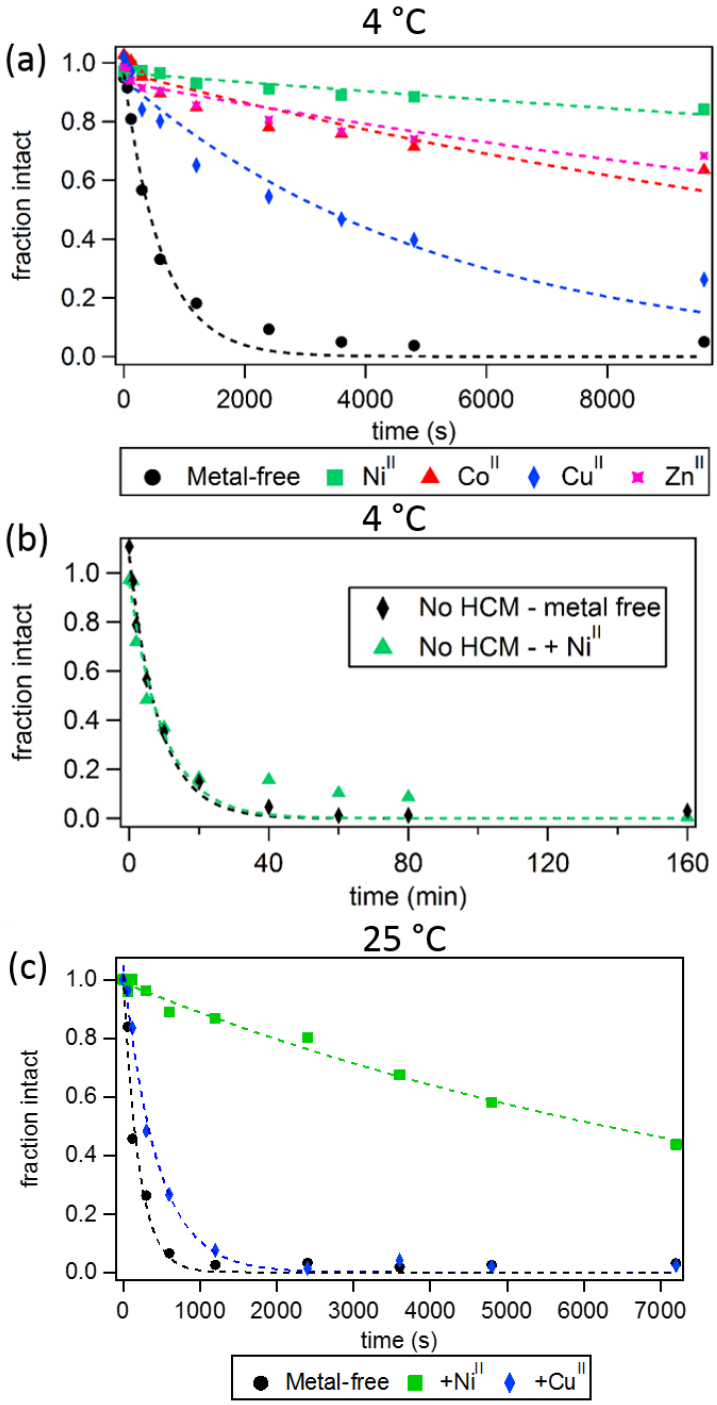

Figure S17. Tryptic digestion of P3 at 4 or 25 °C in the presence and absence of M^{II}. (a) Kinetics of trypsin digestion when P3 was metal-free (black circles), or bound to Cu^{II} (blue diamonds), Co^{II} (red triangles), Zn^{II} (pink squares), or Ni^{II} (green squares). (b) Kinetics of trypsin digestion of $P3_{bare}$ in the presence or absence of Ni^{II}. (c) Kinetics of trypsin digestion of metal-free or metal-bound P3 at 25 °C.

Liquid chromatograph-mass spectrometry (LC-MS) was performed on Thermo Scientific Ultimate 3000 HPLC with a flow rate of 0.4 mL/min, with subsequent introduction into an Orbitrap Elite mass spectrometer with electrospray ionization. Buffer A was water with 0.1% TFA and Buffer B was acetonitrile, and both buffers had 10 mM ammonium acetate. Analysis was performed using the Xcalibur software (Fig. S8). It was observed that the cleaved peptide products eluted at the same time by HPLC.

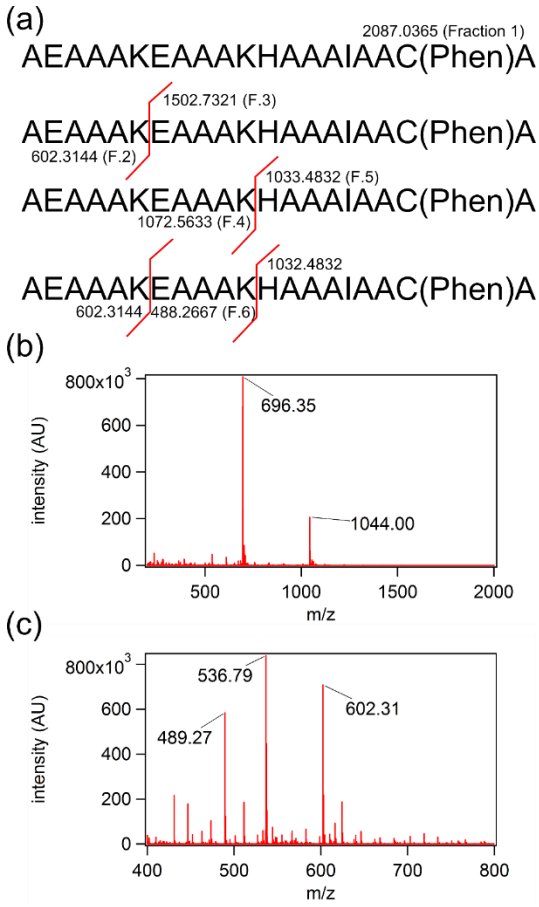

Figure S18. (a) Trypsin cleavage sites and corresponding masses of P3. (b) Masses of intact peptide. Expected molecular weight: 2086.03. Observed: $[M+2H]^{2+}$: 1044.00, expected 1044.02. $[M+3H]^{3+}$: 696.35, expected 696.35. (c) Masses of cleaved peptides. Expected molecular weights: $[M+H]^{+}$: 602.31, observed 602.31. Expected $[M+H]^{+}$: 489.27, observed 489.27. Expected $[M+2H]^{2+}$: 536.79, observed 536.79.

X. CD Spectroscopy of P8

CD experiments were performed using the same conditions as those discussed in Section V.

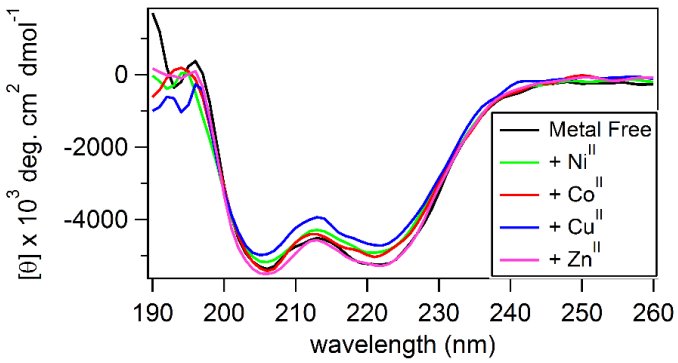

Figure S19. CD spectra of $P8_{bare}$. No change in the helical signal of the peptide was observed upon the addition of metal.

XI. Spectroscopic Dimerization Studies

15 µM peptide solutions were prepared in 20 mM MOPs buffer, pH 7.0. 2 µL aliquots of metal were added, and the samples were monitored either by UV-vis or CD, allowing for at least 3 min of mixing after each addition. The UV-vis signal at 268 and 280 nm was plotted, or the CD signal at 222 nm was plotted, corresponding to the largest spectral changes observed upon metal binding (Fig. S10, S11).

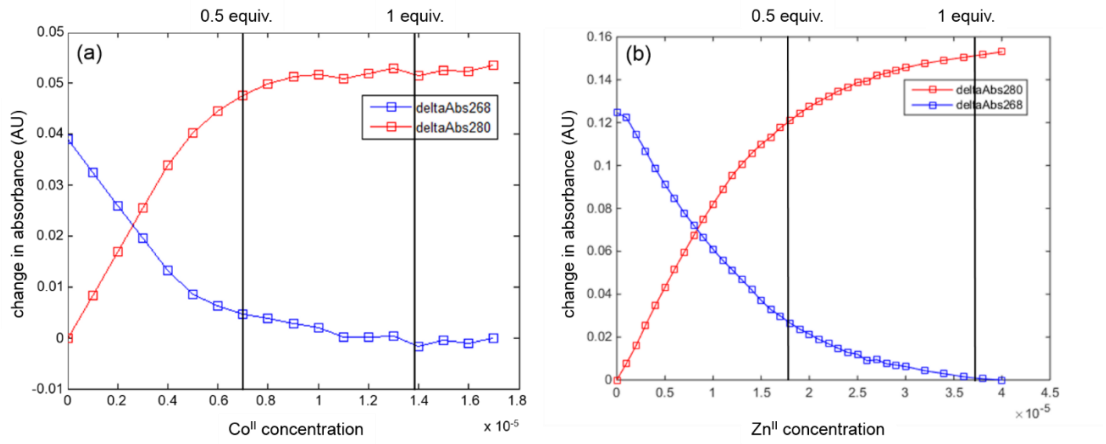

Figure S20. UV-vis titrations to determine the stoichiometry of metal binding and dimer formation. (a) The titration with Co^{II} indicates that the peptide is almost fully dimerized at 0.5 equiv. metal. This is expected given the preference of Co^{II} for octahedral geometry. (b) The titration with Zn^{II} shows some dimer formation, but not to the same extent as Ni^{II} and Co^{II}. (See also Figure 5b)

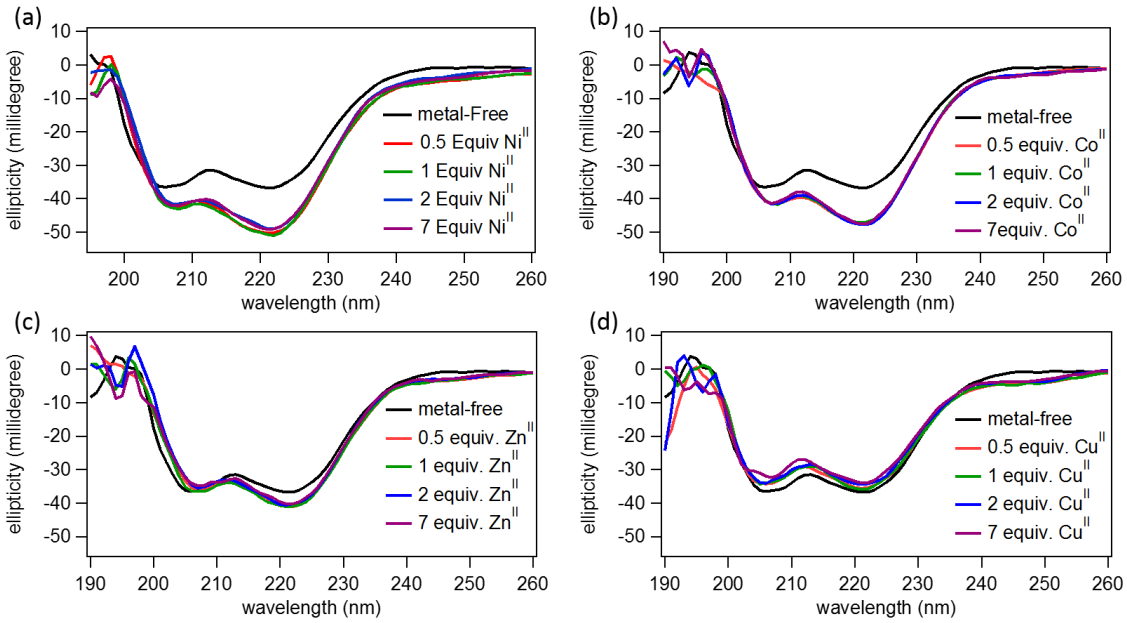

Figure S21. CD titrations to determine the stoichiometry of metal-binding and dimer formation as monitored by CD. Upon the addition of (a) Ni^{II}, (b) Co^{II}, (c) and Zn^{II}, no further change in secondary structure is observed after 0.5 equivalents of M^{II} are added. Very little change is observed upon the addition of (d) Cu^{II}.

XII. Analytical Ultracentrifugation (AUC)

450 µL samples for AUC were prepared with 40 µM peptide in 50 mM MOPs, pH 7. EDTA was used to ensure samples were metal-free, or Ni^{II} was added at either 0.25, 0.5, or 1 equiv. concentration. Measurements were made on a Beckman XL-I Analytical Ultracentrifuge (Beckman-Coulter Instruments) using an An-60 Ti rotor at 60,000 rpm. 400 scans were measured per sample at 25 °C by detection at 270 nm. The data were processed using Sedfit.[14] Buffer viscosity (0.00894 poise), density (0.99764), and protein partial specific volume (0.7132 mL/g) were calculated at 25 °C with SEDNTERP (http://www.jphilo.mailway.com). (See Figure 5c)

XIII. CD Measurements with DNA

Following the same procedure as described in Section V, 5 µM solutions of peptide in 10 mM NaB buffer at pH 7.1 were prepared containing either an excess of EDTA to ensure a metal-free peptide sample, or 0.5 equiv. of M^{II}. After initial CD measurements were conducted, 0.5 equiv. of CRE DNA was added to the solution. After incubating at room temperature for 30 min, the CD spectra was again measured. A sample of DNA-only was measured as well, and this signal was subtracted from that of the DNA-peptide-metal solution (Fig. S12).

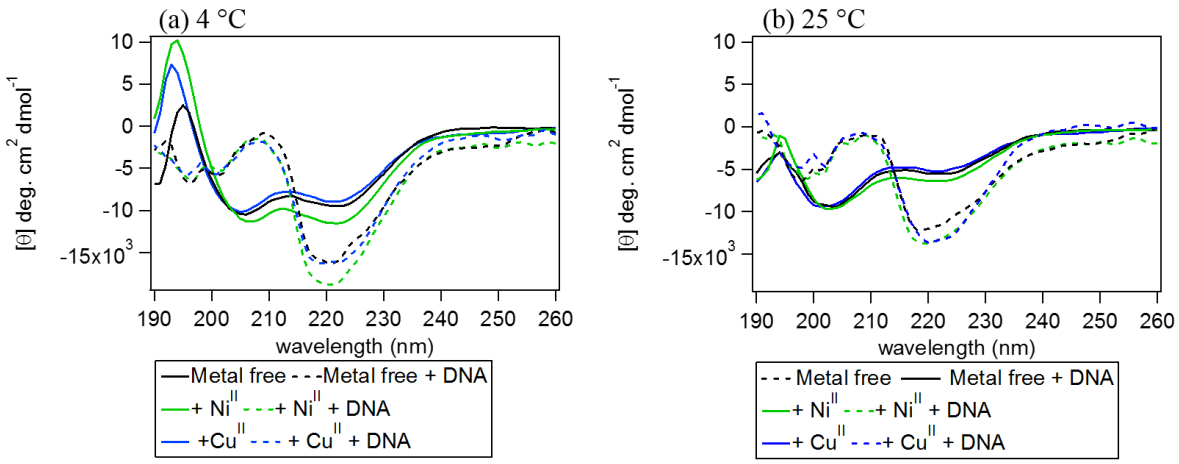

Figure S22. CD spectra of P8 in the presence and absence of M^{II} and DNA.

XIV. Electrophoretic Mobility Shift Assays with Radiolabeled DNA

a. Radiolabeling DNA

1 µL of 20 µM DNA was combined with 2 µL ^{32}P ATP, 1 µL 10x PNK buffer (New England BioLabs), and 5 µL of water in a 0.5 mL Eppendorf tube. 1 µL PNK enzyme (New England BioLabs) was then added and the reaction was incubated at 37 °C for 30 min. At the same time, a 20 x 50 cm 15% polyacrylamide gel, 0.4 mm thick was poured with one large well. After polymerization, the gel was pre-run with 0.5x TBE buffer (44.5 mM Tris base, 44.5 mM boric acid, 1 mM EDTA) at 55 watts for at least 10 min. 30 µL of loading buffer (80% formaldehyde, 20% v/v 5x TBE, bromophenol blue) was added to the DNA reaction mixture and the solution as heated at 80 °C for 2 min. The DNA solution was then loaded into the gel at run at 55 watts for approximately 2 hr, or until the loading dye had run approximately 2/3 the length of the gel.

The location of the radiolabeled DNA was determined using a phosphorimaging plate. The DNA eluted from the gel overnight in water and the supernatant was removed. 30 µL of 3 M sodium acetate, pH 4.9, was added to the supernatant followed by 1.2 mL of ethanol. The solution was incubated at -20 °C for at least 20 min to precipitate DNA. The DNA was then pelleted by centrifugation at 13,200 rpm at 3 °C for 1 hr, and the supernatant was removed. The DNA was then redissolved in 50 µL of water. All waste was disposed of in radioactive waste containers.

b. Electrophoretic Mobility Shift Assays

20-well 8% polyacrylamide gels were made using tris glycine buffer (TG). Samples were prepared with 10 µL binding buffer (20% glycerol, 20 mM Tris, pH 7.5, containing 4 mM $MgCl_2$, 8 mM KCl, 2% NP-40). 18 µL of each sample was loaded and the gel was run for approximately 1.5 hours at 220 milliamps with 1X TG (25 mM Tris-HCl, 250 mM glycine with 0.1% sodium dodecyl sulfate) buffer. In general, the DNA concentration was kept constant at 1 nM while the peptide concentration was varied from 1-500 nM. The metal concentration was maintained at 0.5 equiv. peptide.

Gels were dried under vacuum and imaged using a phosphoimaging plate with overnight exposure. The band intensity was quantified, and the fraction of bound DNA was calculated using the following equation:

Fraction bound = intensity of DNA-peptide band/(intensity of DNA-peptide band + intensity of DNA band)

Dissociation constants were approximated using the following equilibrium equation using Igor Pro for nonlinear least squares regression fitting where P is the peptide, D is the DNA, P_2D is the complex, and P_{tot} is the total peptide added (Fig. S13, S14) (See also Figure 6, Table 3).

$$P + P + D \rightleftharpoons P_2D$$

$$fraction\ bound = \frac{1}{1 + \left(\frac{K_{app}}{P_{tot}}\right)^2}$$

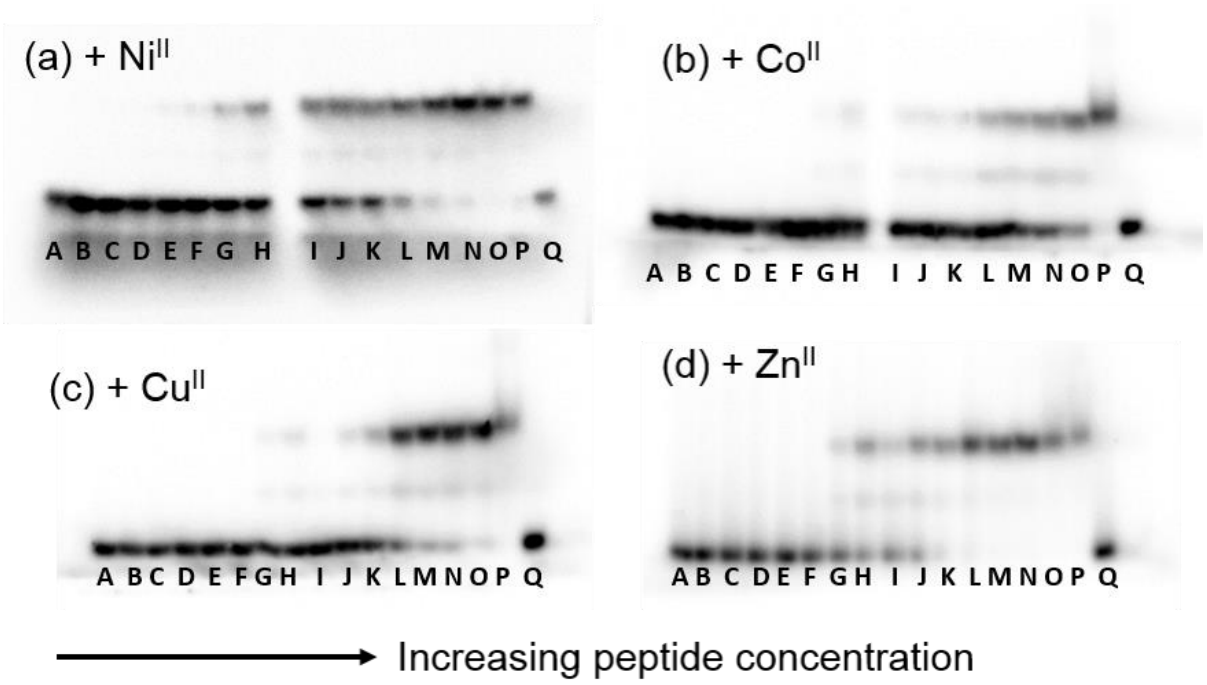

Figure S23. Sample gels from electrophoretic mobility shift assays to observe CRE binding by P8. At some concentrations, an intermediate band is observed that may be due to a peptide monomer bound to the DNA. Lane (Q) contains CRE without any added peptide; DNA concentration is kept constant at 1 nM, while P8 concentration varies: (A) 1 nM, (B) 2 nM, (C) 5 nM, (D) 10 nM, (E) 15 nM, (F) 20 nM, (G) 25 nM, (H) 30 nM, (I) 40 nM, (J) 50 nM, (K) 75 nM, (L) 100 nM, (M) 150 nM, (N) 200 nM, (O) 250 nM, (P) 500 nM.

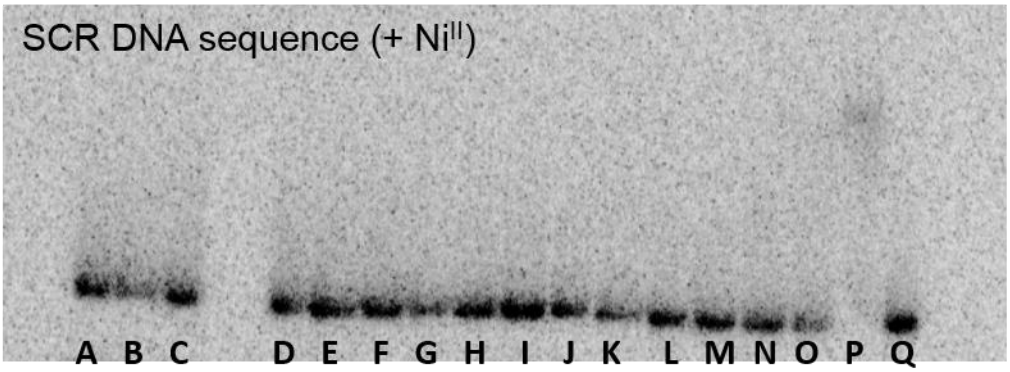

Figure S24. Sample gel shift assays to observe DNA binding by P8 with the SCR DNA sequence. Lane (Q) contains CRE without any added peptide; DNA concentration is kept constant at 1 nM, while P8 concentration varies: (A) 1 nM, (B) 2 nM, (C) 5 nM, (D) 10 nM, (E) 15 nM, (F) 20 nM, (G) 25 nM, (H) 30 nM, (I) 40 nM, (J) 50 nM, (K) 75 nM, (L) 100 nM, (M) 150 nM, (N) 200 nM, (O) 250 nM, (P) 500 nM.

XV. References

(1) Binnemans, K.; Lenaerts, P.; Driesen, K.; Gorller-Walrand, C. *J. Mater. Chem.* **2004**, *14*, 191.
(2) Castellano, F. N.; Dattelbaum, J. D.; Lakowicz, J. R. *Anal. Biochem.* **1998**, *255*, 165.
(3) Radford, R. J.; Nguyen, P. C.; Tezcan, F. A. *Inorg. Chem.* **2010**, *49*, 7106.
(4) Smith, S. J.; Du, K.; Radford, R. J.; Tezcan, F. A. *Chem. Sci.* **2013**, *4*, 3740.
(5) Kuzmic, P. *Anal. Biochem.* **1996**, *237*, 260.
(6) Martell, A. E.; Smith, R. M. *Critical Stability Constants*; Plenum Press: New York, 1974.
(7) Neese, F. *Wiley Interdiscip. Rev.: Comput. Mol. Sci.* **2012**, *2*, 73.
(8) Handy, N. C.; Cohen, A. J. *Mol. Phys.* **2001**, *99*, 403.
(9) Schafer, A.; Horn, H.; Ahlrichs, R. *J. Chem. Phys.* **1992**, *97*, 2571.
(10) Weigend, F.; Ahlrichs, R. *Phys. Chem. Chem. Phys.* **2005**, *7*, 3297.
(11) Sinnecker, S.; Rajendran, A.; Klamt, A.; Diedenhofen, M.; Neese, F. *J. Phys. Chem. A* **2006**, *110*, 2235.
(12) Zhurko, G. A. Z., D.A. **2014**, www.chemcraftprog.com.
(13) John, D. M.; Weeks, K. M. *Protein Sci.* **2000**, *9*, 1416.
(14) Schuck, P. *Biophys. J.* **2000**, *78*, 1606.